



An enhanced grey wolf optimizer boosted machine learning prediction model for patient-flow prediction

Xiang Zhang^a, Bin Lu^b, Lyuzheng Zhang^c, Zhifang Pan^d, Minjie Liao^a, Huihui Shen^a, Li Zhang^e, Lei Liu^f, Zuxiang Li^{g,*}, YiPao Hu^{h,**}, Zhihong Gao^{i,***}

^a Wenzhou Data Management and Development Group Co.,Ltd, Wenzhou, Zhejiang, 325000, China

^b Wenzhou City Bureau of Justice, Wenzhou, Zhejiang, 325000, China

^c B-soft Co.,Ltd., B-soft Wisdom Building No.92 Yueda Lane, Binjiang District, Hangzhou, 310052, China

^d The First Affiliated Hospital of Wenzhou Medical University, Wenzhou, 325000, China

^e Wenzhou Hongsheng Intellectual Property Agency (General Partnership), Wenzhou, Zhejiang, 325000, China

^f College of Computer Science, Sichuan University, Chengdu, Sichuan, 610065, China

^g Organization Department of the Party Committee, Wenzhou University, Wenzhou, 325000, China

^h Wenzhou Health Commission, Wenzhou, Zhejiang, 325000, China

ⁱ Zhejiang Engineering Research Center of Intelligent Medicine, The First Affiliated Hospital of Wenzhou Medical University, Wenzhou, 325000, China



ARTICLE INFO

Keywords:

Patient-flow prediction
Support vector regression
Machine learning
Meta-heuristic
Swarm-intelligence

ABSTRACT

Large and medium-sized general hospitals have adopted artificial intelligence big data systems to optimize the management of medical resources to improve the quality of hospital outpatient services and decrease patient wait times in recent years as a result of the development of medical information technology and the rise of big medical data. However, owing to the impact of several elements, including the physical environment, patient, and physician behaviours, the real optimum treatment effect does not meet expectations. In order to promote orderly patient access, this work provides a patient-flow prediction model that takes into account shifting dynamics and objective rules of patient-flow to handle this issue and forecast patients' medical requirements. First, we propose a high-performance optimization method (SRXGWO) and integrate the Sobol sequence, Cauchy random replacement strategy, and directional mutation mechanism into the grey wolf optimization (GWO) algorithm. The patient-flow prediction model (SRXGWO-SVR) is then proposed using SRXGWO to optimize the parameters of support vector regression (SVR). Twelve high-performance algorithms are examined in the benchmark function experiments' ablation and peer algorithm comparison tests, which are intended to validate SRXGWO's optimization performance. In order to forecast independently in the patient-flow prediction trials, the data set is split into training and test sets. The findings demonstrated that SRXGWO-SVR outperformed the other seven peer models in terms of prediction accuracy and error. As a result, SRXGWO-SVR is anticipated to be a reliable and efficient patient-flow forecast system that may help hospitals manage medical resources as effectively as possible.

1. Introduction

Primary medical care is the guarantee of people's survival and development. With the continuous development of economic, cultural, and social construction, people's demand for medical resources is much

higher. Their awareness of medical and health care also increases requirements for the current medical industry. Since the medical service system is complex, it is not only influenced by factors such as local demographic characteristics, socio-economic conditions, natural environmental conditions, medical hardware, software facilities, and patient

* Corresponding author.

** Corresponding author.

*** Corresponding author.

E-mail addresses: zhxan@126.com (X. Zhang), wzlubin@139.com (B. Lu), 66199293@qq.com (L. Zhang), panzhifang@wmu.edu.cn (Z. Pan), 1829820@qq.com (M. Liao), ylyvias7@126.com (H. Shen), 101744491@qq.com (L. Zhang), liulei.cx@gmail.com (L. Liu), lizuxiang@wzu.edu.cn (Z. Li), huyipao@outlook.com (Y. Hu), gzh@wzhospital.cn (Z. Gao).

and doctor behaviors [1]. But there are also various interactions and positive and negative feedback between these influencing factors, which may result in the longer the waiting time in the hospital, the more attractive the patients are, or the regular changes in the hospital waiting queue, etc. Self-organized regularities and Emergent behavior make it difficult for hospitals to implement optimal outpatient management measures and cause the actual use of available resources not to match the expected results [2]. Therefore, to improve the efficiency of existing medical resources, improve the quality of hospital outpatient services, shorten patient waiting queues and waiting times, it is crucial to understand the changing dynamics and objective patterns of patient-flow to provide a basis for dynamic adjustment of physician consultation plans and to achieve orderly and effective patient control.

In recent years, the advancement of medical informatization and the rise of big medical data has allowed studying patient-flow prediction based on big data mining. Researchers have conducted some research in the analysis of patient-flow change patterns, analysis of patient-flow influencing factors, and patient-flow prediction. Li et al. [3] proposed a time series patient-flow prediction method based on XGBoost, a support vector machine (SVM), to solve the problem of planning and allocation of healthcare resources by government and hospital management. Nikakhtar et al. [4] proposed a patient visit prediction model based on eigendistance and mesocentricity that can help healthcare managers and decision-makers predict the trend of infectious patient-flow. Sharafat et al. [5] proposed an emergency room patient-flow prediction model (PatientFlowNet) based on a deep learning framework, including predicting arrival, treatment, and discharge rates. The results show that PatientFlowNet has higher accuracy and lower average absolute error than the benchmark algorithm. Tavakoli et al. [6] proposed a seasonal autoregressive integrated moving average (SARIMA) model for patient-flow prediction of the current epidemic of neocrown pneumonia disease, effectively predicting the number of patients' visits to Thai hospitals in the next 30. According to the current research status, it is easy to find that more and more researchers are using machine learning techniques to predict the number of patient visits in hospitals. However, since most of the prediction models use a monadic time-series feature prediction method and the changes of patient-flow are affected by a variety of complex factors and do not have obvious linear characteristics, resulting in the accuracy of the models is not high. On the other hand, it is limited by the defects of the classification predictor itself, which leads to large prediction bias of prediction models based on SVM and other prediction models. Therefore, how to improve the accuracy and reduce the error of patient-flow prediction models is a major challenge in current medical resource scheduling research.

As a novel optimization method with strong robustness and flexibility, the swarm intelligence optimization algorithm is widely used in predictive optimization problems. The swarm intelligence optimization algorithm is a stochastic optimization algorithm abstracted by simulating the collaborative behavior of animals, insects, and other organisms. The current well-known algorithms are, grey wolf optimization (GWO) [7], bat-inspired algorithm (BA) [8], differential evolution (DE) [9], sine cosine algorithm (SCA) [10], salp swarm algorithm (SSA) [11], whale optimizer (WOA) [12], moth-flame optimization (MFO) [13], particle swarm optimization (PSO) [14], hunger games search (HGS) [15], Harris hawks optimization (HHO) [16], rime optimization algorithm (RIME) [17], colony predation algorithm (CPA) [18], Runge Kutta optimizer (RUN) [19], weighted mean of vectors (INFO) [20], slime mould algorithm (SMA) [21,22], opposition-based SCA (OBSCA) [23], modified SCA (m SCA) [24], boosted GWO (OBLGWO) [25], A-C parametric WOA (ACWOA) [26], fruit fly optimizer (FOA) with multi-population outpost mechanism (MOFOA) [27], SCA with differential evolution (SCADE) [28], and so on. They also have been applied to solve many problems such as bankruptcy prediction [29], feature selection [30–34], economic emission dispatch [35], multi-objective optimization [36], global optimization [37,38], dynamic multi-objective optimization [39], numerical optimization [40–42],

scheduling optimization [43,44], feed-forward neural networks [45], medical image segmentation [46–48], feature selection [49,50], performance optimization [51,52], identification of pulmonary hypertension animal [53], constrained multi-objective optimization [54], and large-scale complex optimization [55].

More and more researchers are considering optimizing models using swarm intelligence optimization methods to improve the accuracy of prediction methods. Chou et al. [56] proposed a swarm intelligence algorithm-based support vector machine prediction model (SFALSSVM) using the smart firefly algorithm (SFA) to optimize the parameters of the least squares support vector regression (SVR) and successfully applied it to several geotechnical engineering problems. Kaushik et al. [57] proposed a binary swarm intelligence algorithm by combining the firefly algorithm and bat algorithm with a wavelet neural network (WNN) and offered a prediction model for software development effort (SDEE), which has high prediction accuracy. Mehraein et al. [58] proposed a CatBoost (CB) prediction model based on a swarm intelligence algorithm for predicting the monthly flow of satellite precipitation data and demonstrated a significant reduction in the root mean square error (RMSE) of the proposed CB compared with an artificial neural network (ANN). Zhu et al. [59] combined the WOA and the simulated annealing algorithm (SA) to optimize the kernel extreme learning machine (KELM). They proposed an enhanced search-based prediction algorithm (EMWS) that effectively addresses defect prediction in software modules.

Zhou et al. [60] improved the Firefly algorithm (FA) by incorporating chaotic mapping, adaptive inertia weights, and Levy flight for accurate prediction of reinforcement tensile loads for assessing the internal stability of geosynthetic reinforced soil (GRS) structures. They used the improved FA to optimize the hyperparameters of the least-squares SVR model. The improved SVR model had excellent accuracy with an average absolute percentage error of less than 10%. Ma et al. [61] proposed an SVR prediction model integrated with k-fold cross-validation (CV) and used an artificial bee colony (ABC) algorithm and genetic algorithm (GA) to optimize the hyperparameters of the model. The results showed that the hybrid approach can be used to determine the optimal hyperparameters and present statistical significance. Huang et al. [62] proposed a swarm intelligence algorithm (DFP) integrating floral pollination algorithm (FPA) and differential evolution (DE) and an algorithmic model for predicting the groutability of cement paste in combination with SVR. Luo et al. proposed a hybrid prediction model (LS-SVMR) using a coupled simulated annealing (CSA) algorithm to optimize the hyperparameter selection of SVR, which effectively implemented the lateral strength prediction of reinforced concrete (RC) columns.

Based on the above improvement methods for prediction models, it can be found that swarm intelligence optimization algorithms can effectively help prediction models find optimal hyperparameters, and SVR is applied very frequently in many models. However, due to the variety of swarm intelligence algorithms, each algorithm has defects, such as low convergence accuracy, slow search speed, and easy falling into local optimality. Therefore, in this paper, to accurately predict the number of patients and reasonably schedule medical resources, an SVR prediction model based on improved GWO is proposed using the GWO algorithm with high exploitation capability combined with SVR prediction methods. First, to give full play to the exploitation advantages of GWO and overcome the shortcomings of GWO in the search process as much as possible, the following three methods are used for improvement: (1) To address the problem of narrow coverage of the initialized search agent of GWO, the original random initialization method is used instead of Sobol sequence to expand the distribution of the initial solution. (2) To address the problem of too little information exchange among GWO search agents, a directional mutation mechanism is used to increase the interactivity of solutions, improving the algorithm's search efficiency. (3) To address the problem of imbalance between GWO search and exploitation, a Cauchy random replacement strategy is added

to the core update formula to adjust the weights of search and exploitation of the algorithm in the iterative process. Based on the above ideas, Sobol sequence-based population initialization, Cauchy random replacement strategy, and directional mutation mechanism are introduced into GWO to propose a high-performance GWO variant (SRXGWO). Then, to verify the optimization performance of SRXGWO, this paper designs comparative simulation experiments based on the classical IEEE CEC2014 test set and compares SRXGWO with other X methods. The experiments show that the proposed SRXGWO method significantly improves initialization, search efficiency, and defects of iterative balance. This paper also analyzes the comparative results using the Wilcoxon signed-rank test [63] and the Friedman test [64]. SRXGWO has a higher convergence speed compared with peer algorithms and accuracy.

Further, this paper proposes a multivariate SRXGWO-SVR prediction model for predicting patient flow by optimizing two hyperparameters of SVR using high-performance SRXGWO. To validate the real prediction ability of the SRXGWO-SVR model, the prediction results of the model are presented in detail using real clinical data sets and divided into training and test sets. Further, the SRXGWO-SVR model based on SRXGWO, the GWO-SVR model based on GWO, and the original SVR model are compared in this paper, and the experimental results also demonstrate that the SRXGWO-SVR can effectively outperform the two original models without improvement. Finally, this paper also compares the SRXGWO-SVR model with well-known prediction models such as Radial basis function networks, convolutional neural networks, etc. R-squared (R^2), root mean squared error (RMSE), and mean absolute error (MAE) are used for validation and confirm that SRXGWO-SVR is more advantageous in predicting hospital patient-flow. The data set used in this paper is the attendance statistics of Wenzhou Medical University Hospital in China, which serves a radius of nearly 30 million people and has an annual outpatient volume of 5.3 million. Due to the large volume of data, the latest data from January 2022 to September 2022 is selected, with a sample size of 240 items. The main contributions of this paper are as follows.

1. Sobol sequence-based population initialization, Cauchy random replacement strategy, and directional mutation mechanism are introduced into GWO to propose a high-performance algorithm SRXGWO. The strategies and mechanisms employed in this paper can provide a valid reference for the field of evolutionary computation.
2. We designed experiments comparing SRXGWO with 12 similar algorithms to verify the algorithm's improvement ideas and optimization performance. Experiments can effectively demonstrate the performance of SRXGWO's benchmark functions and provide illustrations for their specific applications.
3. SRXGWO is used to optimize the hyperparameters of SVR, and the SRXGWO-SVR multivariate prediction model is proposed and successfully applied to predict patient flow. The proposed model can effectively predict patient flow and provide useful suggestions for hospital management.
4. We designed a comparison experiment between SRXGWO-SVR and eight similar prediction models to verify the effectiveness of the improvement and the accuracy of the prediction. The experiments illustrate that the proposed model has great potential for predicting other time series problems.

The rest of this paper is organized as follows. Section 2 describes the prediction dataset, the original GWO, and SVR. In Section 3, SRXGWO is proposed based on three improvement strategies, and the SRXGWO-SVR model is proposed in conjunction with SVR. In Section 4, benchmark function comparison experiments and simulation prediction comparison experiments are designed. Finally, Section 5 summarizes the work of this paper and illustrates further research directions.

2. Materials and methods

This section introduces the swarm intelligence optimization algorithm GWO and the regression prediction model SVR used in this study.

2.1. Description of GWO algorithm

In the GWO algorithm, grey wolf individuals are divided into four classes: α , β , δ and ω . α is mainly responsible for participating in the decision-making and management of the pack; ω is for other grey wolf individuals; β and δ are for grey wolf individuals with the second highest adaptation level to α . The GWO algorithm focuses on three behaviors: encirclement behavior, hunting behavior, and attack behavior.

1. Encirclement behavior

The first stage of prey predation by grey wolves is to encircle the prey, and the mathematical model can be described by Eq. (1) and Eq. (2).

$$\vec{D} = \left| \vec{C} \cdot \vec{X}_p(t) - \vec{X}(t) \right| \quad (1)$$

$$\vec{X}(t+1) = \vec{X}_v(t) - \vec{A} \cdot \vec{D} \quad (2)$$

where \vec{D} is the distance between the prey and the wolves; $\vec{A} = 2a \cdot \vec{r}_2 - a \cdot \vec{C} = 2 \cdot \vec{r}_2$; \vec{X} is the current location of the wolves; t is the number of current iterations; \vec{X}_p is the location of the prey; r_1, r_2 are random numbers, between $[0, 1]$; $a \in [2, 0]$.

2. Hunting behavior

After a wolf pack surrounds a prey, it will hunt the surrounding prey. If α is the global optimal solution, β is the global second solution, and δ is the global third solution, then the mathematical model of α , β , and δ repositioning can be described by Eqs. (3)–(5).

$$\vec{D}_\alpha = \left| \vec{C}_1 \cdot \vec{X}_\alpha - \vec{X} \right| \quad (3)$$

$$\vec{D}_\beta = \left| \vec{C}_2 \cdot \vec{X}_\beta - \vec{X} \right| \quad (4)$$

$$\vec{D}_\delta = \left| \vec{C}_3 \cdot \vec{X}_\delta - \vec{X} \right| \quad (5)$$

where \vec{D}_α , \vec{D}_β and \vec{D}_δ denote the approximate distances of α , β , and δ from \vec{X} , respectively; \vec{X}_α , \vec{X}_β , \vec{X}_δ denote the position information of α , β , and δ , respectively; \vec{C}_1 , \vec{C}_2 and \vec{C}_3 denote the random vectors, respectively. The current solution \vec{X} and the updated solution $\vec{X}(t+1)$ can be described by Eq. (6)–Eq. (9).

$$\vec{X}_1 = \vec{X}_\alpha - \vec{A}_1 \cdot (\vec{D}_\alpha) \quad (6)$$

$$\vec{X}_2 = \vec{X}_\beta - \vec{A}_2 \cdot (\vec{D}_\beta) \quad (7)$$

$$\vec{X}_3 = \vec{X}_\delta - \vec{A}_3 \cdot (\vec{D}_\delta) \quad (8)$$

$$\vec{X}'(t+1) = \left(\vec{X}_1 + \vec{X}_2 + \vec{X}_3 \right) / 3 \quad (9)$$

where \vec{A}_1 , \vec{A}_2 , and \vec{A}_3 denote random vectors, respectively.

3. Attack behavior

The final stage of the GWO algorithm is the prey attack phase, which can be achieved by adjusting the parameter A . If $|A| \leq 1$, the whole wolf pack approaches the prey (X^*, Y^*) and focuses on the prey; if $|A| > 1$, the whole wolf pack moves away from the prey and looks for new prey again.

2.2. Description of support vector regression

Support vector machine (SVM) models are used to classify data by mapping the input metric data to a higher dimensional space, then constructing an optimal hyperplane in this higher dimensional space so that the constructed hyperplane has the largest edges to classify the input data. The learning strategy used by the support vector machine is interval maximization, which can be formalized as solving a convex quadratic programming problem.

Instead of the traditional statistical induction followed by deduction, the SVR model constructs a regression function to infer a prediction model on the training data and then uses the model to make predictions. The objective of SVR modeling is to build a classification surface that separates the two types of samples as well as possible. SVR modeling aims to minimize the distance between all the sample data and the classification surface. The accuracy of the SVR model is highly dependent on the kernel function's quality and the penalty factor's accuracy, and the appropriate choice of parameters dramatically improves the accuracy of the regression model. When the parameters of the regression model are not selected appropriately, the regression model will not be applicable to solve the actual problem. For the training data, regression aims to solve the following regression function, as in Eq. (10).

$$f(y) = \langle W^0 y \rangle + b \quad (10)$$

The above equation is $\langle w^0 y \rangle$ is the inner product of w and y . The following equation is the constraint to solve the constrained optimization problem:

$$\text{Min } 1 / 2 < w^0 w > + C \sum_{i=1}^m (\xi_i + \xi_i^*) \quad (11)$$

$$Z_i - < w^0 y_i > + b \leq \epsilon + \xi_i \quad (12)$$

$$< w^0 y_i > - z_i + b \leq \epsilon + y_j - y_k \quad (13)$$

where C represents the penalty factor of the model, the value of C is positively related to the complexity of the model, the complexity of the model increases with the value of C , and the value of C is negatively related to the computational error of the model, the error of the model becomes smaller as the value of C increases.

The solution of the optimization problem is first transformed into the corresponding pairwise problem and, secondly transformed into the solution of the maximum constraint value by introducing the kernel function. Finally, the regression equation of the model is shown in Eq. (14).

$$f(y) = \sum_{i=1}^m (a_j - a_j)^0 k(y, y_j) + b \quad (14)$$

3. The proposed method

In this section, three improvement ideas are described, namely, Sobol sequence-based population initialization, Cauchy random replacement strategy, and directional mutation mechanism. Finally, the proposed SRXGWO is used to optimize the hyperparameters of the SVR model, and the patient-flow prediction model SRXGWO-SVR is proposed.

3.1. Proposed GWO variant

3.1.1. Sobol sequence-based population initialization

The population initialization of the original GWO algorithm is randomly generated, which primarily affects the algorithm's performance. In contrast, the Sobol sequence can make the spatial points uniformly distributed and generate unlimited samples without pre-determining the number of samples and storing them. Therefore, this paper introduces the Sobol sequence to filter the initialization position of the grey wolf population, improve the uniformity and diversity of the grey wolf population, and improve the performance of the original GWO algorithm.

Each dimension of the Sobol sequence is a Radical inversion with base 2, and each dimension has a different generating matrix C . When C is taken as a unit vector, the corresponding Sobol sequence is represented as

$$N(i) = \sum_{k=1}^M 2^{-k} ak(i) \quad (15)$$

where i is denoted as a binary number, $ak(i)$ on each bit of the number is arranged as a vector, which is mirrored to the right of the decimal point and converted to decimal, resulting in a one-dimensional Sobol sequence $X_i = \{N(1), N(2), \dots, N(i), i \in N\}$, and a multi-dimensional Sobol sequence is obtained by multiplying the generating matrix C of each dimension. The Sobol sequence is used to uniformly distribute n points within the threshold of the target parameter search as the initialized population space location. The first three solutions are defined as α , β , and δ wolves, respectively. To confirm the effectiveness of Sobol sequence-based population initialization, Ablation experiments of SRXGWO are designed in Section 4.1.2, where SGWO is the improved GWO using this strategy alone.

3.1.2. Cauchy random replacement strategy

In the iterative process, the position update of GWO is conservative. On the one hand, such an update is beneficial to the exploitation of the algorithm. Still, on the other hand, it may cause the algorithm to have a poor quality of the search solution and fall into local optimum when dealing with multi-peaked problems. Therefore, in this paper, to solve this problem, the Cauchy replacement search strategy is used to appropriately perturb the dimensionality of the search agent and improve the interaction between individuals.

Specifically, firstly, the grey wolf population with the number of individuals N is traversed by the parameter l , and the selected one is the X_l individual. Then, according to the ratio of the remaining runs of the algorithm to the total number of runs compared with the Cauchy random number, if the Cauchy random number is less than the ratio, the h -th dimensional value of X_l is replaced with the h th dimensional value of the optimal solution α wolves. Finally, the fitness value of the updated X_l The evaluation function calculates the optimal solution, and the optimal fitness value are replaced if the fitness value is better than the optimal solution. Otherwise, it remains unchanged. To confirm the effectiveness of the Cauchy replacement search strategy, RGWO in Ablation experiments of SRXGWO is the GWO improved using this strategy alone.

3.1.3. Directional mutation strategy

Since the original GWO relies too much on the searchability of the top three ranked wolves to find the optimal solution, it is easy to fall into the local optimal trap and reduce the accuracy of the optimal solution. Therefore, this paper proposes a directional mutation strategy based on genetic algorithms' mutation and crossover strategies. The directional mutation strategy consists of two important operations: directional crossover and directional variation.

1. Directional crossover (DM)

The when-directed crossover mechanism uses the position information of the current iteration's optimal individual to guide the individual's next change trend. There are four main parameters, which are crossover rate (p_c), variable crossover probability (p_{cv}), directional probability (p_d) and multiplication factor (α). First, the execution of the directed crossover mechanism requires different parent individuals in the current population. The parent individuals are generated by random selection from the population, p_1^j and p_2^j , $j \in [1, d]$. p_{mean}^j and p_{best}^j are the mean value of the parent individuals in the j th dimension and the value of the best individual in the j th dimension, respectively. In the first case, when $p_{best}^j \geq p_{mean}^j$ (c_1 and c_2 does the directed hybridization mechanism generate the individuals).

$$val = 1 - 0.5^e \left[\frac{|p_1^j - p_2^j|}{(y_u^j - y_l^j)} \right] \quad (16)$$

$$\beta = \frac{r_3}{\alpha^2} \quad (17)$$

$$c_1 = val * (p_1^j - p_2^j) + \alpha^{r_3} * e^{(1-\beta)} * (1 - val) * |p_1^j - p_2^j|, \text{ if } r_4 \leq p_d \quad (18)$$

$$c_2 = (1 - val) * (p_1^j - p_2^j) - \alpha^{(1-r_3)} * e^{(-\beta)} * val * |p_1^j - p_2^j|, \text{ if } r_4 \leq p_d \quad (19)$$

$$c_1 = val * (p_1^j + p_2^j) - \alpha^{r_3} * e^{(1-\beta)} * (1 - val) * |p_1^j - p_2^j|, \text{ if } r_4 > p_d \quad (20)$$

$$c_2 = (1 - val) * (p_1^j + p_2^j) + \alpha^{(1-r_3)} * e^{(-\beta)} * val * |p_1^j - p_2^j|, \text{ if } r_4 > p_d \quad (21)$$

When $p_{best}^j < p_{mean}^j$.

$$c_1 = val * (p_1^j + p_2^j) - \alpha^{r_3} * e^{(1-\beta)} * (1 - val) * |p_1^j - p_2^j|, \text{ if } r_4 \leq p_d \quad (22)$$

$$c_2 = (1 - val) * (p_1^j + p_2^j) + \alpha^{(1-r_3)} * e^{(-\beta)} * val * |p_1^j - p_2^j|, \text{ if } r_4 \leq p_d \quad (23)$$

$$c_1 = val * (p_1^j + p_2^j) + \alpha^{r_3} * e^{(1-\beta)} * (1 - val) * |p_1^j - p_2^j|, \text{ if } r_4 > p_d \quad (24)$$

$$c_2 = (1 - val) * (p_1^j + p_2^j) - \alpha^{(1-r_3)} * e^{(-\beta)} * val * |p_1^j - p_2^j|, \text{ if } r_4 > p_d \quad (25)$$

If the parent individuals have the same value, but $p_{best}^j \neq p_{mean}^j$.

$$val = 1 - 0.5^e \left[\frac{|p_{best}^j - p_{mean}^j|}{(y_u^j - y_l^j)} \right] \quad (26)$$

$$\beta = \frac{r_3}{\alpha^2} \quad (27)$$

$$c_1 = val * (p_{best}^j + p_{mean}^j) + \alpha^{r_3} * e^{(1-\beta)} * (1 - val) * (p_{best}^j - p_{mean}^j), \text{ if } r_4 \leq p_d \quad (28)$$

$$c_2 = (1 - val) * (p_{best}^j + p_{mean}^j) - \alpha^{(1-r_3)} * e^{(-\beta)} * val * (p_{best}^j - p_{mean}^j), \text{ if } r_4 \leq p_d \quad (29)$$

$$c_1 = val * (p_{best}^j + p_{mean}^j) - \alpha^{r_3} * e^{(1-\beta)} * (1 - val) * (p_{best}^j - p_{mean}^j), \text{ if } r_4 > p_d \quad (30)$$

$$c_2 = (1 - val) * (p_{best}^j + p_{mean}^j) + \alpha^{(1-r_3)} * e^{(-\beta)} * val * (p_{best}^j - p_{mean}^j), \text{ if } r_4 > p_d \quad (31)$$

where r_3 and r_4 are two different random numbers, $r_3 \in (0, 1)$ and $r_4 \in (0, 1)$. val and β are two parameters computed in each iteration. y_u^j and y_l^j are the upper and lower bounds of the individual in the j th dimension, respectively. A is the multiplicative factor.

2. Directional variation

First, assume that the dimensions of population size and objective function are D and d , respectively. Assume that the current iteration individual is y . The guided variation mechanism guides the variation of the current iteration individual y based on the position information of the current optimal individual y_{best} . When individual y is selected for guided mutation operation, the DM mechanism will compare the size of y_i^j and y_{best}^j , if $y_{best}^j \geq y_i^j$.

$$\beta_1 = e^{\left(\frac{2r - 2}{r} \right)} \quad (32)$$

$$\beta_2 = e^{\left(\frac{r - 2}{r} \right)} \quad (33)$$

$$y_m = \begin{cases} y_i^j + \beta_1 * (y_u^j - y_i^j), & \text{if } r_2 \leq p_d \\ y_i^j - \beta_2 * (y_i^j - y_l^j), & \text{otherwise} \end{cases} \quad (34)$$

where β_1 and β_2 are two parameters, which can also be called the weights that determine the change steps of the formula. r and r_2 are two random numbers, $r \in (0, 1)$ and $r_2 \in (0, 1)$, $r \neq 0$. y_u^j and y_l^j are the upper and lower bounds of the individual in the j th dimension, respectively. p_d represents the orientation probability, $p_d \in (0.5, 1)$. If $y_{best}^j < y_i^j$.

$$y_m = \begin{cases} y_i^j - \beta_1 * (y_i^j - y_l^j), & \text{if } r_2 \leq p_d \\ y_i^j + \beta_2 * (y_u^j - y_i^j), & \text{otherwise} \end{cases} \quad (35)$$

To illustrate the effectiveness of the Directional mutation strategy, the XGWO in ablation experiments of SRXGWO is the GWO improved using this strategy alone.

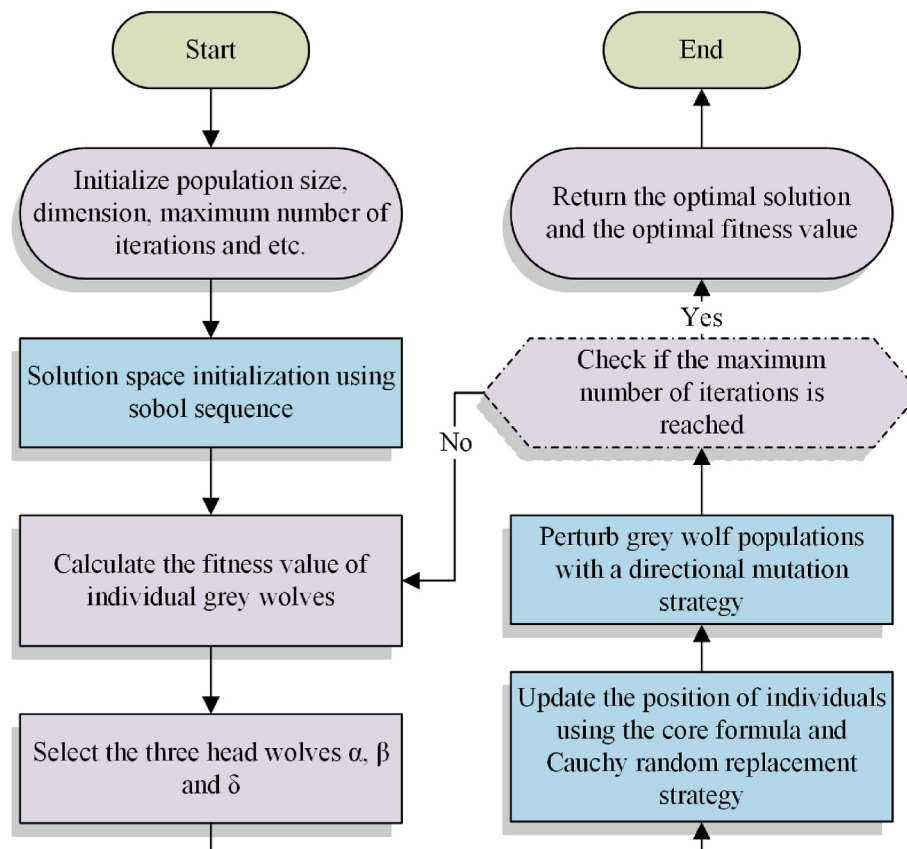
3.1.4. Proposed SRXGWO

The analysis shows that GWO is an excellent algorithm with solid exploitation capability, but several aspects still need improvement. First, GWO is randomly generated with strong uncertainty in the initialization of the grey wolf population, which will lead to the initial solution of the whole population cannot effectively cover the solution space of the problem, thus causing problems such as low efficiency in the search phase. Secondly, the lack of information exchange among individuals in the iterative process of GWO tends to make the algorithm suffer from poor-quality of search solutions and fall into local optimum when dealing with multi-peaked problems. In addition, GWO relies too much on the exploitation ability of the top three ranked wolves to find the optimal solution, which cannot effectively search the whole solution space, leading to the inability to find the optimal solution and reducing the quality of understanding.

Therefore, this paper addresses the above three problems and makes corresponding improvements to GWO. First, Sobol sequence-based population initialization is used instead of the original random initialization method to generate a low-sequence population of grey wolves, which covers the whole solution space uniformly. Second, the dimensional values between search agents are effectively exchanged by Cauchy's random replacement strategy to enhance the information exchange between individuals and improve the exploitation capability of the algorithm. Third, the directional mutation mechanism is introduced to perform crossover and mutation at the level of the search solution, and the crossover or mutation operation is performed for the nature of the current individuals, which effectively improves the search ability of the algorithm and the ability to jump out of the local optimum. The algorithm flowchart of SRXGWO as shown in Fig. 1.

3.2. The proposed SRXGWO-SVR model

To accurately predict the number of patients and reasonably schedule medical resources, this section combines the high-performance

**Fig. 1.** Algorithm flow chart of SRXGWO

The algorithmic complexity of SRXGWO comes mainly from Sobol sequences, core formula updates, Cauchy random replacement strategy, and directional mutation mechanism. The complexity level of Sobol sequence initialization is $O(N)$; the computational complexity level of the core formula is $O(N^2 + N * \log N)$; the computational complexity level of Cauchy random replacement strategy is $O(N * \log N)$; and the complexity level of directional mutation mechanism is $O(N^2)$. By comprehensive calculation, the overall complexity level of SRXGWO is $O(\text{SRXGWO}) = O(N^2 + N * \log N)$.

SRXGWO algorithm with the SVR prediction method and proposes the SRXGWO-SVR, an SVR prediction model based on the improved GWO.

According to Section 2.2, SVR is a supervised machine learning method with two key parameters: the penalty parameter C and the kernel function parameter γ . The penalty parameter C affects the complexity and stability of the model, the kernel function parameter reflects the distribution of samples in the feature space, and the parameter selection directly impacts the prediction accuracy and generalization ability of the model. Therefore, to address the above issues, SRXGWO is introduced to optimize the radial basis kernel function parameters and penalty factors in the SVR patient-flow prediction model to form the best combination of parameters to improve the prediction accuracy and reduce the error size. The specific steps for building the SRXGWO-SVR model are as follows.

- (1) Data pre-processing. Routine data pre-processing is performed on the collected patient-flow data, including data cleaning, missing value processing, outlier processing, etc.
- (2) Establish the objective function. The sample data are substituted into the mean square error minimization function as shown in Eq. (26), and then the optimal radial basis kernel function parameters C and penalty factor γ are obtained.

$$Q = m(C, \sigma) = \frac{1}{n} \sum_{k=1}^n (y_k - \hat{y}_k)^2 \quad s.t. \quad C \in [C_{\min}, C_{\max}], \gamma \in [\gamma_{\min}, \gamma_{\max}] \quad (36)$$

where y_k denotes the actual size of the patient flow, and \hat{y}_k denotes the corresponding size value of the patient-flow prediction.

- (3) Search for hyperparameters using SRXGWO. First, the parameters involved in the SRXGWO algorithm are set initially. The fitness function RMSE is applied to calculate the fitness values of the population individuals, where m is the number of samples.

$$RMSE = \sqrt{\frac{1}{m} \sum_{k=1}^m (y_k - \hat{y}_k)^2} \quad (37)$$

- (4) Determine whether the maximum number of iterations is reached. The iteration is continued if the maximum number of iterations is not reached. Suppose the maximum number of iterations is reached. In that case, the C and γ corresponding to the optimal individual location information is output. The best combination of the two parameters is applied to build the SRXGWO-SVR prediction model. Then the patient-flow dataset is predicted.

The flow chart of the SRXGWO-SVR prediction model based on hospital patient-flow proposed in this section is shown in Fig. 2.

4. Experimental results and discussions

In this section, ablation and benchmark function experiments are designed to validate the global optimization performance of SRXGWO. Then, the proposed SRXGWO-SVR is used in patient-flow prediction experiments to demonstrate the accuracy and validity of SRXGWO-SVR.

4.1. Benchmark functions comparison experiment

4.1.1. Benchmark test experiment setup

First, the running environment of the benchmark function test experiment needs to be described. the software of the experiment is Matlab2017b and the core hardware is Intel(R) Xeon(R) CPU E5-2660v3 (2.60 GHz). The benchmark function test set used in this section is the currently familiar IEEE CEC2014, described in detail in Table 1. The comparison experiments include SRXGWO and GWO and well-known

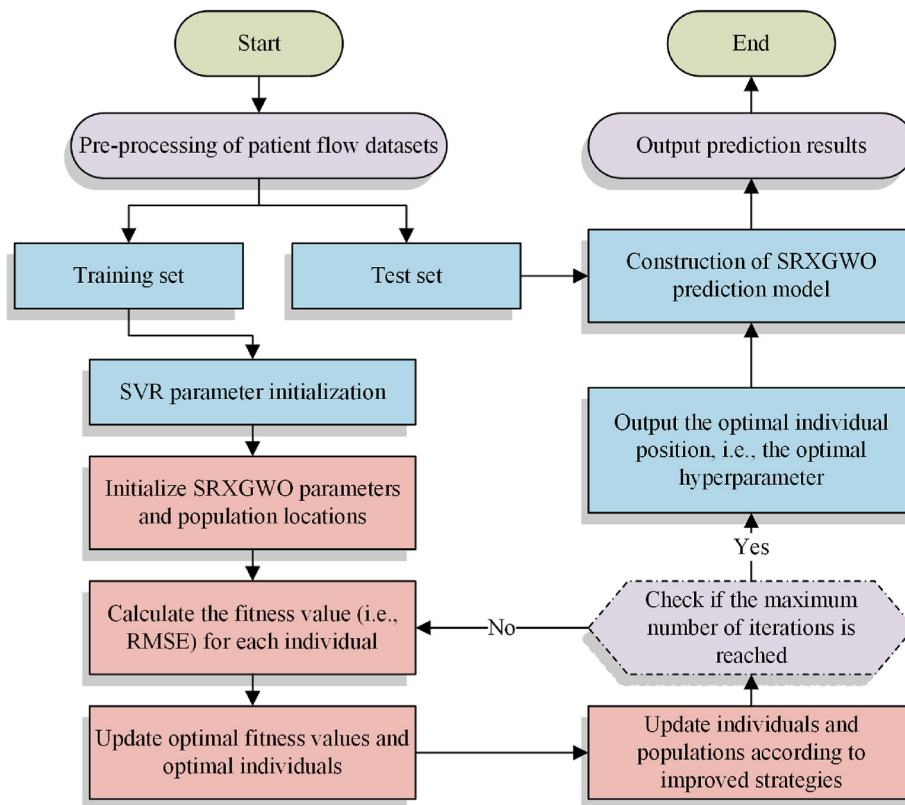


Fig. 2. SRXGWO-SVR prediction model based on hospital patient-flow.

algorithms such as PSO, SCA, etc. Therefore, to ensure the validity and fairness of the experiments, all swarm intelligence algorithms are searched in dimension 30, the population size is 30, the number of evaluations is also uniformly 300,000, and the internal parameters of the algorithms are all default values. Finally, to ensure the correctness and validity of the experimental results, all the algorithms were run independently 30 times, and the results of the experiments were further verified using Wilcoxon signed-rank test and the Friedman test.

4.1.2. Ablation experiments

In this section, ablation experiments of SRXGWO were designed to discuss the effects of Sobol sequence-based population initialization, Cauchy random replacement strategy, and directional mutation mechanism on the effect of GWO. First, the experiments combined the three improved strategies with GWO by permutation, including GWO itself, with a total of eight algorithms, as shown in Table 2. In the table, S stands for Sobol sequence-based population, R stands for Cauchy random replacement strategy, and X stands for directional mutation mechanism. in addition, “1” indicates that the current strategy is used, and “0” indicates that no strategy is used. For example, SGWO uses the Sobol sequence but not the other two strategies.

Table 3 shows the experimental results of SRXGWO with the other seven algorithms, including the Wilcoxon signed-rank test results and P-value. The number of algorithms that are “better than/equal to/worse than” other algorithms. “Mean” indicates the average ranking of the 30 functions tested, and “rank” indicates the final overall ranking. In the results of the Wilcoxon test, SRXGWO is 23 better than the unimproved GWO, which indicates that the improvement of GWO by the three improvement strategies is very significant. In addition, SRXGWO has a significant advantage over SGWO, RGWO, and XGWO using a single mechanism, with at least 14 stronger than them. Finally, SRXGWO has an advantage over the two-two combination of SRGWO, SXGWO, and RXGWO, indicating that the three SRXGWO improvement strategies are effective. The table also shows the empirical p-values, and the bolded

data indicate that SRXGWO is significantly different from other algorithms, and it can be said that the advantage of SRXGWO is more prominent compared to other algorithms. In summary, the mechanism employed in SRXGWO is reasonable and effective, and can significantly improve the performance of GWO.

4.1.3. Comparison of SRXGWO with well-known peer algorithms

In this subsection, similar algorithm comparison experiments are designed based on 30 benchmark functions to compare SRXGWO with 12 other peer algorithms to demonstrate that the proposed algorithm has more robust optimization performance among the same type of algorithms. Among the compared algorithms, six original algorithms are PSO, SCA, MFO, WOA, BA, and FA, all highly cited algorithms. The other six algorithms are new variants proposed recently, including OBSCA, mSCA, OBLGWO, ACWOA, MOFOA, and SCADE.

Table 4 shows the experimental results of the comparison. Where AVG denotes the average optimal fitness value of 30 independent experiments, STD denotes the variance of the experiments, and the bolded data are the optimal values of the current function of the algorithm. In the experimental results, SRXGWO finds the optimal solution relative to its peer algorithms in most of the function evaluations, especially in the class of complex functions F23–F30, which indicates that SRXGWO is more advantageous in dealing with complex problems. In addition, the STD fluctuation of SRXGWO is small, which suggests that the algorithm has strong stability.

Similarly, to further validate the SRXGWO experimental results, we used the Wilcoxon signed-rank test to compare and validate SRXGWO, and the results are shown in Table 5; the Friedman test was used to verify the average ranking of SRXGWO, and the results are shown in Fig. 3, which can be more intuitive to observe the comparison results. The Wilcoxon signed-rank test results show that SRXGWO ranks first overall when comparing other algorithms and is at least 19 better than other high citation algorithms and 20 better than other variants. The Friedman test shows that the average ranking of SRXGWO is slightly different, but

Table 1

Description of the 30 benchmark functions.

Class	No.	Functions	$F_i^* = F_i(x^*)$
Simple Multimodal Functions	1	Rotated High Conditioned Elliptic Function	100
	2	Rotated Bent Cigar Function	200
	3	Rotated Discus Function	300
	4	Shifted and Rotated Rosenbrock's Function	400
	5	Shifted and Rotated Ackley's Function	500
	6	Shifted and Rotated Weierstrass Function	600
	7	Shifted and Rotated Griewank's Function	700
	8	Shifted Rastrigin's Function	800
	9	Shifted and Rotated Rastrigin's Function	900
	10	Shifted Schwefel's Function	1000
	11	Shifted and Rotated Schwefel's Function	1100
	12	Shifted and Rotated Katsuura Function	1200
	13	Shifted and Rotated HappyCat Function	1300
	14	Shifted and Rotated HGBat Function	1400
	15	Shifted and Rotated Expanded Griewank's plus Rosenbrock's Function	1500
	16	Shifted and Rotated Expanded Scaffer's F6 Function	1600
Hybrid Functions	17	Hybrid Function 1 ($N = 3$)	1700
	18	Hybrid Function 2 ($N = 3$)	1800
	19	Hybrid Function 3 ($N = 4$)	1900
	20	Hybrid Function 4 ($N = 4$)	2000
	21	Hybrid Function 5 ($N = 5$)	2100
	22	Hybrid Function 6 ($N = 5$)	2200
Composition Functions	23	Composition Function 1 ($N = 5$)	2300
	24	Composition Function 2 ($N = 3$)	2400
	25	Composition Function 3 ($N = 3$)	2500
	26	Composition Function 4 ($N = 5$)	2600
	27	Composition Function 5 ($N = 5$)	2700
	28	Composition Function 6 ($N = 5$)	2800
	29	Composition Function 7 ($N = 3$)	2900
	30	Composition Function 8 ($N = 3$)	3000

Table 2

GWO variants based on three strategies.

Algorithms	S	R	X
SRXGWO	1	1	1
GWO	0	0	0
SGWO	1	0	0
RGWO	0	1	0
XGWO	0	0	1
SRGWO	1	1	0
SXGWO	1	0	1
RXGWO	0	1	0

it is still better than PSO and MFO algorithms, and the overall performance is also the first. In summary, the results of the comparison experiment are valid and reasonable, and SRXGWO does outperform other peer algorithms.

To further demonstrate the advantages of SRXGWO over other algorithms, this experiment recorded the optimization search process of each algorithm and plotted it as an iterative curve, as shown in Fig. 4. The horizontal coordinate indicates the number of evaluations, and the vertical coordinate indicates the fitness value. Firstly, it can be seen that SRXGWO has good convergence accuracy on F6, F8, F9, F10, F11 and F13 in unimodal and simple multimodal function classification and faster search speed than other similar algorithms. In addition, it can be observed in the hybrid and combinatorial functions F16, F23, F30 that SRXGWO also has excellent results in solving complex optimization problems. Further in the figure, SRXGWO has a clear advantage in the F6, F8, F9, F10, and F16 test functions. Both in the search period of the search process and the exploitation period of the iteration, SRXGWO can quickly find the current optimal solution. At the same time, the other

algorithms cannot outperform SRXGWO from the beginning to the end. In addition, SRXGWO has a clear decreasing inflection point in the middle of the algorithm iteration in the function tests of F11 and F16. Few other algorithms can continue the development, which indicates that SRXGWO has a strong ability to jump out of the local optimum. Finally, the nine function tests in the figure demonstrate that SRXGWO has stronger search and exploitation capabilities than other algorithms and is a high-performance optimization algorithm. In future work, it also be applied to more cases, such as optimization of machine learning models [65], MRI reconstruction [66], service ecosystem [67], computational experiments [68,69], power distribution network [70], and medical signals [71,72].

4.2. Patient-flow prediction

The patient-flow dataset is presented in this section, and SRXGWO-SVR training and test experiments are designed. First, the patient flow dataset used is presented. Immediately after, the experimental setup including comparison methods, parameter settings, and evaluation criteria are described. Finally, SRXGWO-SVR is proposed and applied to the prediction of patient flow.

4.2.1. Patient-flow dataset

The data set used in this section is the attendance statistics of Wenzhou Medical University Hospital in China, which serves a radius of nearly 30 million people and has an annual outpatient volume of 5.3 million. Due to the large volume of data, the latest data from January 2022 to September 2022 is selected, with a sample size of 240 items. The data's main characteristic attribute is "number of appointments," and the label attribute is "number of actuals". In addition, to reduce the dependence of the model on a single time series and the error of the prediction results, this paper also selects three independent attribute series, namely, "number of people without pre-deposit system", "number of people without ID", and "number of late arrivals". "Three independent attribute series are selected to describe the trend changes of patient-flow with the influence of multiple factors. Finally, when collecting data, there are inevitably null values and outliers, and this paper also preprocesses the data by removing abnormal samples and linear interpolation. Fig. 5 shows a 240-day line graph of actual hospital visits.

First of all, according to Fig. 5, we can see that the number of hospital visits as a whole fluctuates a lot, and there is a local repetition, mostly between 14,000 and 4,200 visits. The main reason for this phenomenon is that the 14,000 visits are during the weekdays, i.e., Monday through Friday, when the hospital doctors are in regular attendance and the equipment is functioning normally, and the number of visits is relatively higher. The 4,200 visits are due to the fact that most of the departments and facilities are closed during the weekends, and the number of visits is relatively low. In addition, it can be seen that the average number of hospital visits between 180 and 220 days was very high, reaching 18,000 at one point, and the number of weekend visits did not drop too much. This is because this period corresponds to July and August, which is the free time of summer vacation, and most people will concentrate on their visits during this period. In general, this data set shows a cyclical distribution, and the difficulty in building the model is to reduce the error while avoiding the problem of overfitting.

4.2.2. Experimental setup

First, the numerical settings of the SRXGWO and GWO algorithms used for hyperparameter optimization are presented. The number of populations is set to 20, the dimension is defined as 2, the maximum number of iterations is 50, the upper and lower bounds for the value of C are 100 and 0.1, and the upper and lower bounds for the value of R are also 100 and 0.1. Then, to prove the effectiveness of the prediction model SRXGWO-SVR improvement, the SRXGWO-SVR was compared with GWO-SVR and the original SVR in the experiments. Also, to prove the effectiveness of SRXGWO-SVR model, backpropagation (BP),

Table 3

Results of Wilcoxon signed-rank test for ablation experiments and P-value.

Item	SRXGWO	GWO	SGWO	RGWO	XGWO	SRGWO	SXGWO	RXGWO
+/-/ =	~	23/1/6	15/1/14	14/3/13	18/0/12	6/5/19	9/0/21	9/2/19
Mean	2.57	6.90	5.40	4.47	4.67	2.93	4.13	3.53
Rank	1	8	7	5	6	2	4	3
F1	N/A	1.9209E-06	1.0246E-05	4.0483E-01	4.7162E-02	2.8948E-01	9.7772E-02	1.6503E-01
F2	N/A	1.9209E-06	1.9209E-06	8.3071E-04	1.6394E-05	2.4118E-04	3.7243E-05	3.3269E-02
F3	N/A	1.7344E-06	1.7344E-06	6.0350E-03	8.9364E-01	6.8359E-03	6.2683E-02	3.1849E-01
F4	N/A	2.3704E-05	3.8822E-06	6.2884E-01	3.6094E-03	4.4052E-01	7.8647E-02	5.9994E-01
F5	N/A	1.7344E-06	2.6033E-06	6.8923E-05	1.7344E-06	4.1955E-04	1.7344E-06	8.1302E-01
F6	N/A	4.7162E-02	3.1618E-03	7.0356E-01	4.4052E-01	9.0993E-01	9.0993E-01	9.0993E-01
F7	N/A	1.7344E-06	1.7344E-06	1.1499E-04	1.2453E-02	4.0715E-05	3.1618E-03	6.5833E-01
F8	N/A	1.7344E-06	1.9209E-06	9.3676E-02	1.7344E-06	1.9861E-01	2.3534E-06	7.1889E-01
F9	N/A	3.6004E-01	2.9894E-01	2.4308E-02	8.6121E-01	5.5774E-01	2.2888E-01	7.0356E-01
F10	N/A	1.7344E-06	1.7344E-06	4.7162E-02	2.1266E-06	4.7162E-02	1.9209E-06	6.2884E-01
F11	N/A	7.3433E-01	3.0861E-01	5.0383E-01	4.1653E-01	1.3591E-01	9.2626E-01	5.5774E-01
F12	N/A	8.2206E-02	5.4401E-01	5.9836E-02	3.3173E-04	7.7309E-03	1.1079E-02	3.6004E-01
F13	N/A	2.2102E-01	3.9333E-01	1.8462E-01	5.5774E-01	2.9894E-01	3.1849E-01	4.1653E-01
F14	N/A	1.3975E-02	1.8326E-03	2.6230E-01	8.5896E-02	1.2544E-01	1.7791E-01	2.3694E-01
F15	N/A	1.4773E-04	6.3391E-06	3.6826E-02	4.9080E-01	2.7653E-03	1.8462E-01	1.0201E-01
F16	N/A	5.3197E-03	2.9575E-03	1.1138E-03	7.5213E-02	2.5637E-02	1.7138E-01	6.5641E-02
F17	N/A	9.8421E-03	3.0861E-01	3.1849E-01	8.7297E-03	3.8723E-02	7.1889E-01	6.5833E-01
F18	N/A	6.8359E-03	9.3157E-06	8.5896E-02	8.9187E-05	6.5641E-02	1.4936E-05	1.4773E-04
F19	N/A	1.4839E-03	8.9443E-04	1.9861E-01	6.4352E-01	1.3591E-01	2.0589E-01	2.1827E-02
F20	N/A	1.9209E-06	1.7344E-06	5.3070E-05	5.3044E-01	5.2165E-06	1.5886E-01	7.3433E-01
F21	N/A	9.0993E-01	4.7795E-01	7.5213E-02	1.0639E-01	2.1827E-02	8.2901E-01	5.0383E-01
F22	N/A	1.6503E-01	6.5641E-02	7.1903E-02	1.6503E-01	3.8203E-01	1.8519E-02	2.4519E-01
F23	N/A	1.7344E-06	1.0000E+00	1.7344E-06	1.7344E-06	1.0000E+00	1.0000E+00	1.7344E-06
F24	N/A	1.7344E-06	1.0000E+00	1.7344E-06	1.7344E-06	1.0000E+00	1.0000E+00	1.7344E-06
F25	N/A	1.2290E-05	1.0000E+00	1.7344E-06	5.6061E-06	1.0000E+00	1.0000E+00	1.7344E-06
F26	N/A	1.9729E-05	1.6566E-02	1.0357E-03	1.3820E-03	1.5286E-01	3.1603E-02	3.1618E-03
F27	N/A	1.7344E-06	1.0000E+00	1.7344E-06	1.7344E-06	1.0000E+00	1.0000E+00	1.7344E-06
F28	N/A	1.7344E-06	1.0000E+00	1.7344E-06	1.7344E-06	1.0000E+00	1.0000E+00	1.7344E-06
F29	N/A	1.7344E-06	1.0000E+00	1.7344E-06	1.7344E-06	1.0000E+00	1.0000E+00	1.7344E-06
F30	N/A	1.7344E-06	1.0000E+00	1.7344E-06	1.7344E-06	1.0000E+00	1.0000E+00	1.7344E-06

random forest (RF), KELM, radial basis function network (RBF), convolutional neural networks (CNN), and other well-known predictive classifiers are added to the comparison experiments. To verify the prediction effectiveness of the proposed patient-flow prediction models, three evaluation metrics are applied to evaluate the performance of various prediction models in this paper. The three-evaluation metrics are the spearman correlation coefficient (R^2) of Eq. (38), the mean absolute error (MAE) of Eq. (39), and the root mean square error (RMSE) of Eq. (40) for the evaluation analysis.

$$R^2 = 1 - \frac{\sum_{k=1}^m (y_k - \hat{y}_k)^2}{\sum_{k=1}^m (\bar{y}_k - \hat{y}_k)^2} \quad (38)$$

$$MAE = \frac{1}{m} \sum_{i=0}^{m-1} |y_i - \hat{y}_i| \quad (39)$$

$$RMSE = \sqrt{\frac{1}{n} \sum_{k=1}^m (y_k - \hat{y}_k)^2} \quad (40)$$

where m is the number of samples, y_k is defined as the actual value size of the test sample, \bar{y}_k is the mean size of the test sample, and \hat{y}_k is the predicted value of the test sample.

4.2.3. Prediction results and analysis

To perform regression calculations on the decomposed subsequences using the SVR model, the patient-flow data set needs to meet the input format of the SVR model. For this purpose, the original data samples are processed as follows.

First, for the time series y_1, y_2, \dots, y_n , define the input matrix.

$$X = \begin{bmatrix} y_1 & \cdots & y_d \\ \vdots & \ddots & \vdots \\ y_{n-d} & \cdots & y_{n-1} \end{bmatrix} \quad (41)$$

where d is the step size parameter and is the number of sample attributes, which in this paper is 4.

Then, define the output labels.

$$y = \begin{bmatrix} y_{d+1} \\ \vdots \\ y_n \end{bmatrix} \quad (42)$$

Finally, use X and y defined above as the input and label of the SVR model, respectively. In practice, X and y are divided into a training set and a test set in the ratio of 1:1. The training set is used to train the model and determine the optimal parameters of the model. Then, the trained model is simulated and tested on the test set to demonstrate the training effect of the prediction model. Finally, the accuracy performance of the model is verified by evaluating the metrics R^2 , RMSE, and MAE. The following are the experimental results and training and test sets analysis.

1. Prediction experiments on the training set

The patient-flow dataset is divided into 120 sample sets by 1:1 crossover as the training set for training seven prediction models, including SRXGWO-SVR, GWO-SVR, SVR, BP, RF, KELM, RBF, and CNN.

Fig. 6 shows the prediction result plot of SRXGWO-SVR. The original fold represents the training set's original data distribution and the Predicted fold represents the prediction results given by the SRXGWO-SVR model. The line graph shows that the overall prediction effect of the SRXGWO-SVR model is excellent, especially in the interval of 70–120 days. The Original and Predicted lines nearly overlap, which indicates that the prediction is very accurate. The large deviations between the

Table 4

Comparison results of SRXGWO with other algorithms.

Fun	F1	F2	F3		
Item	AVG	STD	AVG	STD	AVG
SRXGWO	1.5817E+07	8.9158E+06	1.7773E+08	1.4681E+08	4.5005E+03
PSO	9.0808E+06	1.6903E+06	1.4837E+08	1.5123E+07	9.9378E+02
SCA	2.2839E+08	6.9799E+07	1.6889E+10	2.3915E+09	3.7046E+04
MFO	8.7549E+07	1.0414E+08	1.0114E+10	5.9855E+09	1.0275E+05
WOA	2.7540E+07	1.1331E+07	5.0637E+06	8.0209E+06	3.2575E+04
BA	7.7059E+05	3.5272E+05	5.2698E+05	2.7431E+05	4.2251E+02
FA	2.5269E+08	5.1675E+07	1.5002E+10	1.8122E+09	6.4325E+04
OBSCA	4.0160E+08	1.2958E+08	2.4801E+10	4.7138E+09	5.0550E+04
m_SCA	6.3874E+07	4.1104E+07	6.3318E+09	3.7149E+09	2.6908E+04
OBLGWO	2.2042E+07	1.2605E+07	1.6887E+07	1.2778E+07	9.1358E+03
ACWOA	1.3860E+08	6.2461E+07	7.4290E+09	3.9581E+09	5.0191E+04
MOFOA	1.2354E+09	7.4867E+07	7.7038E+10	2.4594E+09	7.8687E+04
SCADE	4.5429E+08	1.1842E+08	3.0003E+10	4.0210E+09	5.6160E+04
Fun	F4		F5		F6
Item	AVG	STD	AVG	STD	AVG
SRXGWO	5.4006E+02	3.2112E+01	5.2075E+02	7.2959E-02	6.1118E+02
PSO	4.6707E+02	3.2003E+01	5.2095E+02	4.0216E-02	6.2317E+02
SCA	1.4150E+03	2.7588E+02	5.2093E+02	6.2064E-02	6.3356E+02
MFO	1.5209E+03	1.0125E+03	5.2030E+02	1.6938E-01	6.2361E+02
WOA	5.9251E+02	6.0017E+01	5.2034E+02	1.6112E-01	6.3494E+02
BA	4.2155E+02	3.2061E+01	5.2095E+02	6.4791E-02	6.3398E+02
FA	1.5337E+03	1.5192E+02	5.2096E+02	4.5044E-02	6.3359E+02
OBSCA	2.3121E+03	7.5405E+02	5.2095E+02	5.7443E-02	6.3205E+02
m_SCA	8.0286E+02	1.1489E+02	5.2056E+02	1.4351E-01	6.2212E+02
OBLGWO	5.4647E+02	4.7860E+01	5.2096E+02	5.9910E-02	6.1916E+02
ACWOA	1.1803E+03	2.6266E+02	5.2085E+02	1.7768E-01	6.3363E+02
MOFOA	1.0092E+04	6.9816E+02	5.2106E+02	3.7558E-02	6.4079E+02
SCADE	2.2480E+03	4.6553E+02	5.2097E+02	4.3335E-02	6.3428E+02
Fun	F7		F8		F9
Item	AVG	STD	AVG	STD	AVG
SRXGWO	7.0144E+02	4.4844E-01	8.3494E+02	6.4659E+00	9.9741E+02
PSO	7.0229E+02	1.4348E-01	9.7268E+02	2.6092E+01	1.1067E+03
SCA	8.4528E+02	2.6369E+01	1.0362E+03	1.9353E+01	1.1756E+03
MFO	7.9627E+02	6.3419E+01	9.4824E+02	3.3320E+01	1.1205E+03
WOA	7.0099E+02	7.2969E-02	9.9955E+02	4.1935E+01	1.1246E+03
BA	7.0066E+02	1.6102E-01	1.0275E+03	5.2626E+01	1.1641E+03
FA	8.4000E+02	1.0997E+01	1.0240E+03	1.2118E+01	1.1595E+03
OBSCA	9.1758E+02	4.4244E+01	1.0576E+03	1.8074E+01	1.1960E+03
m_SCA	7.4867E+02	2.2125E+01	9.3470E+02	2.3339E+01	1.0491E+03
OBLGWO	7.0119E+02	9.2779E-02	9.2058E+02	3.4783E+01	1.0637E+03
ACWOA	7.3883E+02	2.1566E+01	9.8681E+02	1.5413E+01	1.1270E+03
MOFOA	1.4082E+03	4.6569E+01	1.1760E+03	1.1881E+01	1.2583E+03
SCADE	9.1691E+02	4.4469E+01	1.0684E+03	1.0564E+01	1.2058E+03
Fun	F10		F11		F12
Item	AVG	STD	AVG	STD	AVG
SRXGWO	1.7815E+03	2.3016E+02	4.1565E+03	1.0677E+03	1.2012E+03
PSO	5.0248E+03	5.6761E+02	5.8289E+03	4.4923E+02	1.2023E+03
SCA	7.0064E+03	5.2529E+02	8.0775E+03	3.0696E+02	1.2025E+03
MFO	4.6021E+03	8.7516E+02	5.2295E+03	7.7681E+02	1.2004E+03
WOA	4.9691E+03	7.4150E+02	5.8744E+03	9.0861E+02	1.2017E+03
BA	5.5034E+03	5.6881E+02	6.0313E+03	6.9746E+02	1.2011E+03
FA	7.5532E+03	3.1957E+02	7.9058E+03	2.9315E+02	1.2026E+03
OBSCA	6.3076E+03	4.9831E+02	7.3709E+03	3.6056E+02	1.2022E+03
m_SCA	4.0584E+03	7.1133E+02	4.7823E+03	6.5478E+02	1.2008E+03
OBLGWO	3.8703E+03	8.9566E+02	5.4446E+03	1.0838E+03	1.2023E+03
ACWOA	4.7309E+03	7.3276E+02	6.1655E+03	9.3475E+02	1.2018E+03
MOFOA	9.2300E+03	3.9968E+02	9.0883E+03	2.8283E+02	1.2029E+03
SCADE	7.3914E+03	2.4356E+02	8.2418E+03	2.8346E+02	1.2026E+03
Fun	F13		F14		F15
Item	AVG	STD	AVG	STD	AVG
SRXGWO	1.3004E+03	7.4709E-02	1.4005E+03	2.8662E-01	1.5163E+03
PSO	1.3004E+03	7.7571E-02	1.4003E+03	1.2817E-01	1.5166E+03
SCA	1.3030E+03	2.6429E-01	1.4439E+03	7.6871E+00	5.5707E+03
MFO	1.3020E+03	1.3201E+00	1.4347E+03	2.4514E+01	2.1529E+05
WOA	1.3006E+03	1.4348E-01	1.4003E+03	4.2398E-02	1.5738E+03
BA	1.3005E+03	1.5518E-01	1.4003E+03	1.3344E-01	1.5296E+03
FA	1.3028E+03	1.9987E-01	1.4404E+03	4.2258E+00	1.4383E+04

(continued on next page)

Table 4 (continued)

Fun	F1	F2	F3	
OBSCA	1.3037E+03	3.6249E-01	1.4731E+03	1.1450E+01
m_SCA	1.3009E+03	7.5448E-01	1.4172E+03	7.0904E+00
OBLGWO	1.3005E+03	1.1306E-01	1.4004E+03	1.7893E-01
ACWOA	1.3015E+03	1.0565E+00	1.4197E+03	1.4944E+01
MOFOA	1.3081E+03	3.0417E-01	1.6411E+03	9.7254E+00
SCADE	1.3040E+03	3.7540E-01	1.4874E+03	8.7317E+00
Fun	F16		F17	
Item	AVG	STD	AVG	STD
SRXGWO	1.6110E+03	4.7850E-01	6.0312E+05	7.0192E+05
PSO	1.6120E+03	5.3328E-01	2.9096E+05	1.3413E+05
SCA	1.6127E+03	2.3363E-01	6.2791E+06	3.3409E+06
MFO	1.6128E+03	4.8942E-01	3.9449E+06	7.4952E+06
WOA	1.6124E+03	4.0816E-01	4.2933E+06	3.4224E+06
BA	1.6133E+03	3.0344E-01	1.0170E+05	9.2079E+04
FA	1.6129E+03	2.1659E-01	6.7984E+06	1.7537E+06
OBSCA	1.6130E+03	2.5196E-01	9.4571E+06	3.4434E+06
m_SCA	1.6114E+03	7.5109E-01	1.7735E+06	1.3758E+06
OBLGWO	1.6120E+03	4.3556E-01	1.2085E+06	9.3079E+05
ACWOA	1.6122E+03	4.8843E-01	1.5272E+07	1.2808E+07
MOFOA	1.6134E+03	2.3187E-01	8.7256E+07	2.6488E+07
SCADE	1.6127E+03	2.0380E-01	1.5384E+07	5.7531E+06
Fun	F19		F20	
Item	AVG	STD	AVG	STD
SRXGWO	1.9173E+03	1.3658E+01	2.9079E+03	1.1572E+03
PSO	1.9172E+03	1.9835E+00	2.2959E+03	6.5024E+01
SCA	1.9893E+03	2.5079E+01	1.5103E+04	3.7270E+03
MFO	1.9738E+03	5.5538E-01	5.2933E+04	4.0442E+04
WOA	1.9384E+03	2.7102E+01	3.2328E+04	2.0050E+04
BA	1.9335E+03	3.4019E-01	2.4023E+03	1.1992E+02
FA	2.0050E+03	1.2211E+01	1.8924E+04	7.2016E+03
OBSCA	2.0080E+03	9.9922E+00	2.9021E+04	1.1924E+04
m_SCA	1.9502E+03	2.9621E-01	1.0791E+04	4.6890E+03
OBLGWO	1.9170E+03	1.6997E+01	5.6962E+03	2.3328E+03
ACWOA	2.0080E+03	2.5161E-01	3.9788E+04	1.9571E+04
MOFOA	2.2412E+03	1.8281E+01	1.4788E+05	5.3365E+04
SCADE	2.0087E+03	1.1766E+01	2.8049E+04	9.6164E+03
Fun	F22		F23	
Item	AVG	STD	AVG	STD
SRXGWO	2.6550E+03	1.8361E+02	2.5000E+03	0.0000E+00
PSO	2.9439E+03	1.8435E+02	2.6161E+03	5.8346E-01
SCA	2.9644E+03	1.3112E+02	2.6653E+03	1.3746E+01
MFO	3.0695E+03	2.1885E-02	2.6708E+03	3.4130E+01
WOA	3.0538E+03	2.9728E+02	2.6334E+03	1.0652E+01
BA	3.3420E+03	4.1760E+02	2.6152E+03	3.0962E-03
FA	3.0002E+03	1.1217E+02	2.7329E+03	1.7512E+01
OBSCA	3.1226E+03	1.6474E+02	2.6858E+03	1.7839E+01
m_SCA	2.6046E+03	2.1219E+02	2.6370E+03	6.7666E+00
OBLGWO	2.7106E+03	1.7350E+02	2.6181E+03	1.4048E+00
ACWOA	3.1046E+03	2.2793E+02	2.5122E+03	4.6578E+01
MOFOA	1.8112E+04	1.1960E+04	2.5000E+03	0.0000E+00
SCADE	3.1435E+03	1.3870E+02	2.5000E+03	0.0000E+00
Fun	F25		F26	
Item	AVG	STD	AVG	STD
SRXGWO	2.7000E+03	0.0000E+00	2.7004E+03	8.2706E-02
PSO	2.7118E+03	7.4419E-00	2.7871E+03	3.4604E+01
SCA	2.7269E+03	8.2372E+00	2.7023E+03	6.7894E-01
MFO	2.7194E+03	1.1345E+01	2.7024E+03	1.2575E+00
WOA	2.7153E+03	1.6594E-01	2.7005E+03	1.3903E-01
BA	2.7314E+03	1.2072E+01	2.7005E+03	1.5158E-01
FA	2.7336E+03	3.7833E+00	2.7024E+03	3.2727E-01
OBSCA	2.7000E+03	1.4243E-08	2.7040E+03	4.1439E-01
m_SCA	2.7124E+03	4.1923E+00	2.7008E+03	2.1587E-01
OBLGWO	2.7000E+03	0.0000E+00	2.7006E+03	1.2740E-01
ACWOA	2.7000E+03	0.0000E+00	2.7636E+03	4.8645E+01
MOFOA	2.7000E+03	0.0000E+00	2.7925E+03	2.3425E+01
SCADE	2.7000E+03	0.0000E+00	2.7070E+03	1.7566E+01
Fun	F28		F29	
Item	AVG	STD	AVG	STD

(continued on next page)

Table 4 (continued)

Fun	F1		F2		F3	
SRXGWO	3.0000E+03	0.0000E+00	3.1000E+03	0.0000E+00	3.2000E+03	0.0000E+00
PSO	6.8849E+03	8.7157E+02	7.4382E+04	1.3763E+05	1.1678E+04	6.2526E+03
SCA	4.7736E+03	2.6752E+02	1.2836E+07	7.6163E+06	2.3980E+05	7.9328E+04
MFO	3.9703E+03	2.4525E+02	3.6610E+06	3.9023E+06	6.3694E+04	5.2942E+04
WOA	5.0223E+03	6.7902E+02	6.3246E+06	4.5803E+06	7.5080E+04	4.8586E+04
BA	5.1296E+03	5.6070E+02	3.6448E+07	2.6098E+07	1.3731E+04	1.2024E+04
FA	4.2282E+03	1.4435E+02	3.1490E+06	8.4923E+05	1.7420E+05	3.9597E+04
OBSCA	5.3567E+03	2.9466E+02	2.0712E+07	9.7835E+06	3.7443E+05	1.9299E+05
m_SCA	3.8890E+03	1.2875E+02	1.9729E+06	4.4218E+06	5.5540E+04	2.8810E+04
OBLGWO	3.4266E+03	5.0458E+02	4.9452E+06	4.3781E+06	1.9074E+04	1.4566E+04
ACWOA	4.3232E+03	1.2224E+03	1.8950E+07	1.5200E+07	3.7383E+05	2.2958E+05
MOFOA	3.0000E+03	0.0000E+00	3.1000E+03	0.0000E+00	3.2000E+03	0.0000E+00
SCADE	4.9933E+03	8.5262E+02	1.5512E+07	9.5368E+06	4.8922E+05	1.6393E+05

Table 5
Wilcoxon signed-rank test results of SRXGWO versus other peers.

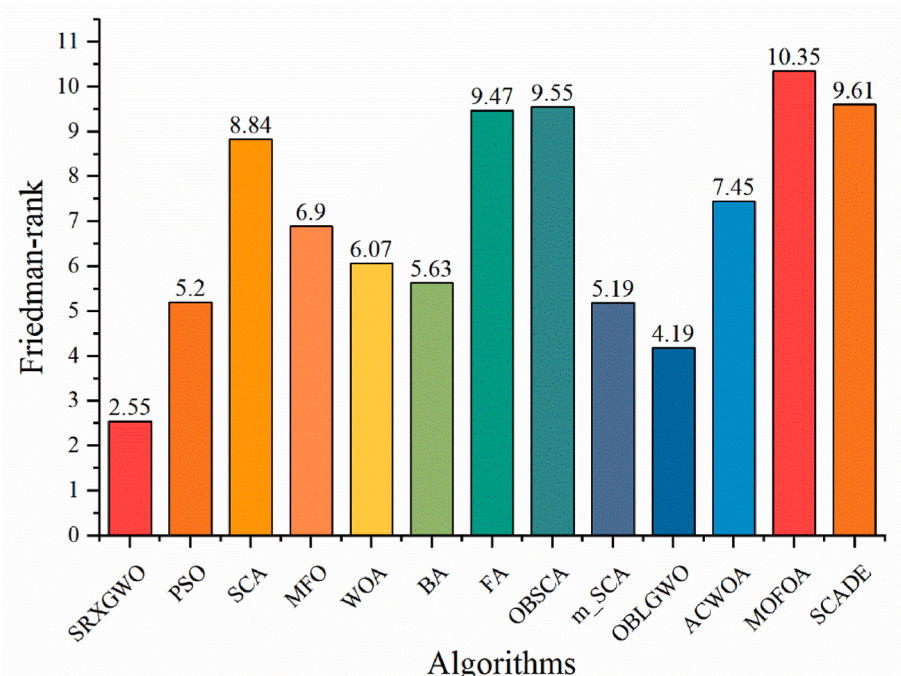
Algorithm	+/-/ =	Mean	Rank
SRXGWO	~	2.13	1
PSO	19/8/3	4.80	4
SCA	30/0/0	8.57	9
MFO	26/2/2	7.33	7
WOA	25/4/1	6.13	6
BA	20/7/3	5.93	5
FA	30/0/0	9.47	10
OBSCA	29/0/1	9.70	11
m_SCA	26/2/2	4.73	3
OBLGWO	20/2/8	4.00	2
ACWOA	28/0/2	7.57	8
MOFOA	23/0/7	10.17	13
SCADE	27/0/3	9.87	12

real and predicted series appear on the 3rd day, around the 32nd day, etc., due to the large fluctuations of the real series, which are difficult to predict and lead to the deviation of the model.

To illustrate the improvement of SRXGWO-SVR compared to GWO-SVR, the iteration curves when SRXGWO and GWO optimized SVR are recorded in this paper, as shown in Fig. 7. The vertical axis represents

the fitness value of the swarm intelligence algorithm, i.e., the deviation in the model, and the horizontal axis represents the number of iterations. The blue curve represents the iteration curve of SRXGWO-SVR, and the brown curve represents the iteration curve of GWO-SVR. The iterations also confirm that the two hyperparameters of the SRXGWO-SVR prediction model are C = 76.2569 and R = 0.0101. The hyperparameters of the GWO-SVR are C = 2.3654 and R = 0.0309. Since the overall deviations of both SRXGWO-SVR and GWO-SVR are small, and the process of iteration spans an extensive numerical range, we have enlarged the key parts were enlarged. First, in terms of initialization, SRXGWO-SVR has a smaller fitness value than GWO-SVR, which indicates that the Sobol sequence initialization method enhances the pre-search capability of SRXGWO. Then, it can be seen by the magnified image that both SRXGWO and GWO find the near-optimal solution at the iteration number of 2, but it is evident that SRXGWO has a better fitness value for the near-optimal solution. Finally, during the iterations, SRXGWO also keeps searching for the optimal solution, and the fitness value of SRXGWO is optimized from 0.0003285 at the beginning to 0.0003271. The fitness value of GWO does not change significantly, and the algorithm falls into a local optimum. Therefore, it can be said that SRXGWO can improve SVR's prediction performance more effectively than GWO.

This work compares SRXGWO-SVR with well-known classification prediction models including GWO-SVR, SVR, BP, RF, KELM, RBF, and

**Fig. 3.** Friedman test results of SRXGWO versus other peers.

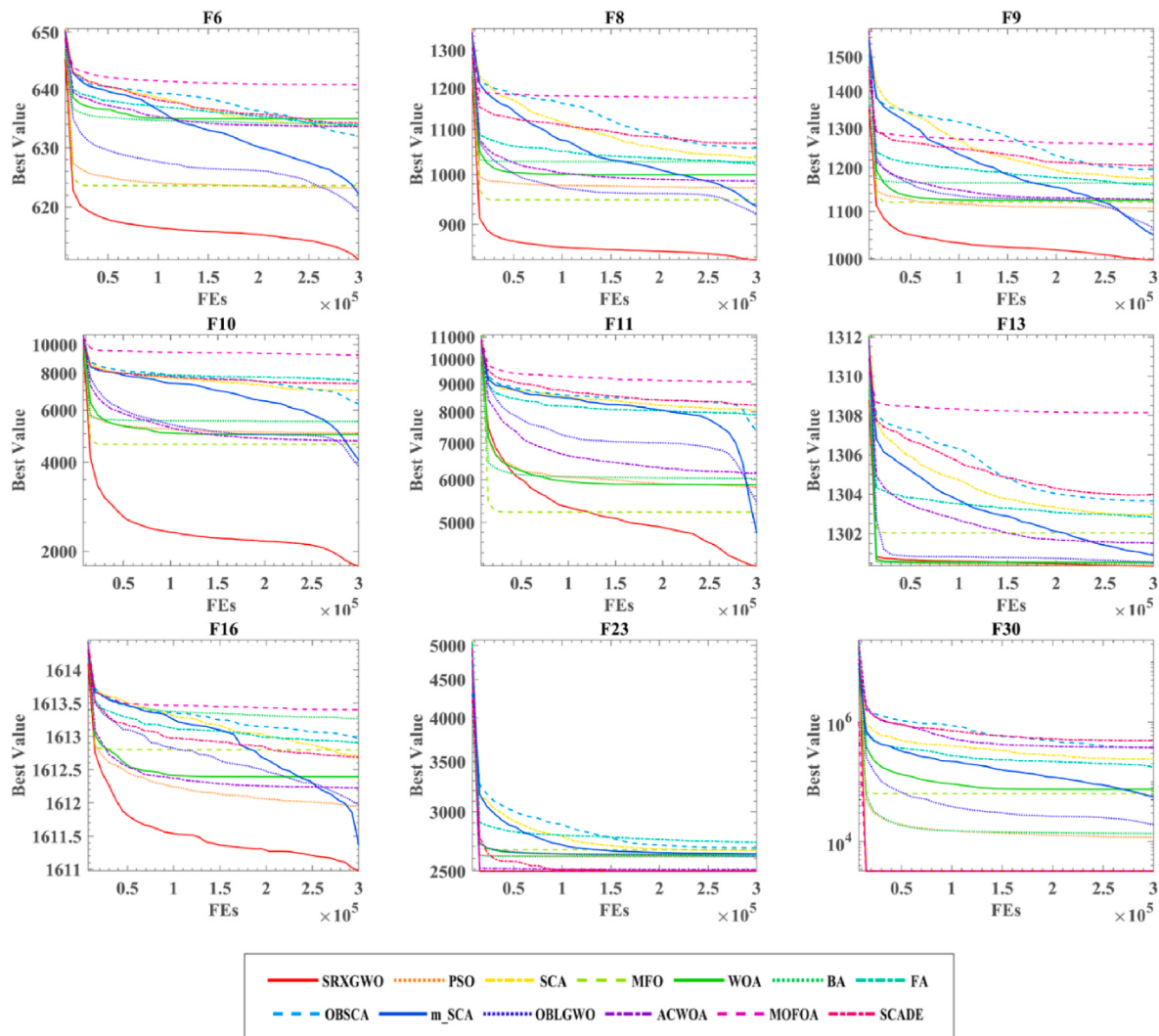


Fig. 4. Convergence curves of SRXGWO and peer algorithms.

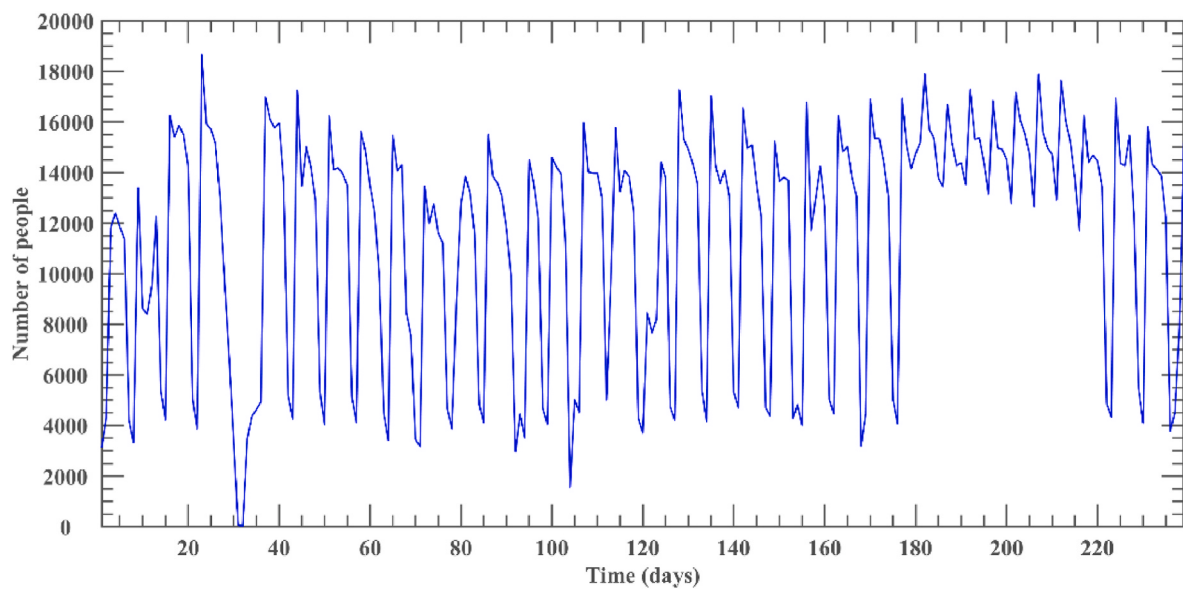


Fig. 5. 240-day folding graph of the number of actual hospital visits.

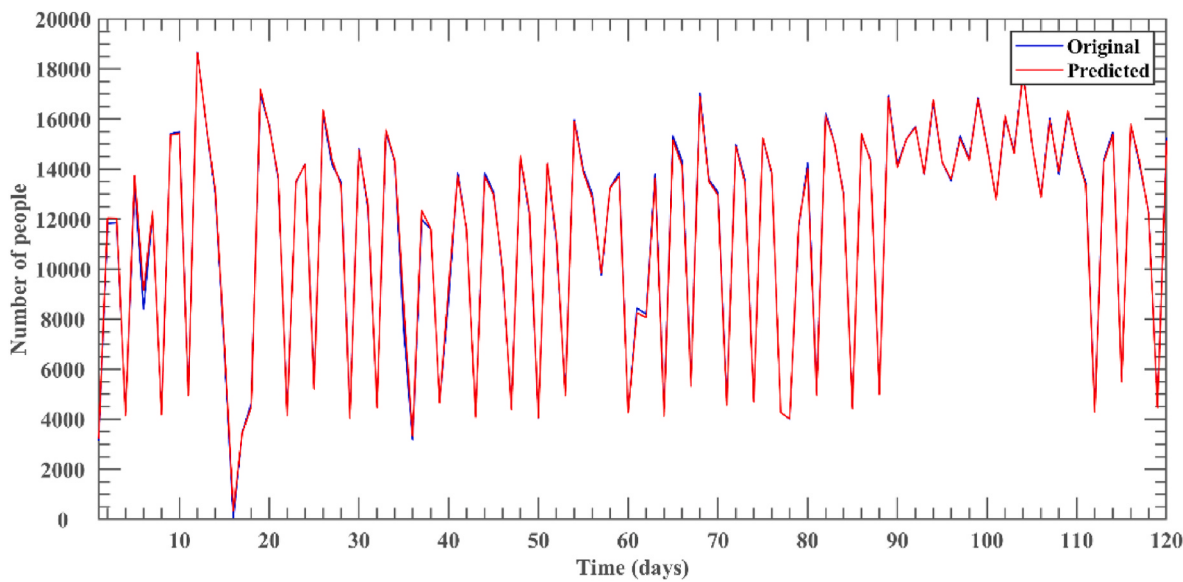


Fig. 6. Prediction results of SRXGWO-SVR.

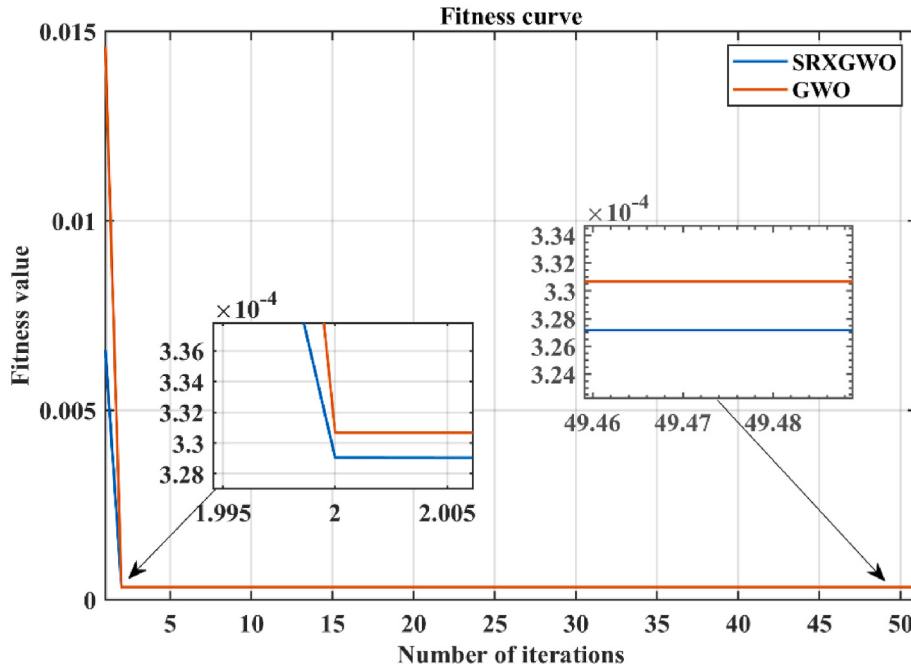


Fig. 7. Iteration curves of SRXGWO and GWO when optimizing SVR.

CNN to further highlight the benefits of SRXGWO-SVR. It uses R^2 , RMSE, and MAE to assess the accuracy of the predictions. In order to guarantee the stability of the prediction results and prevent chance mistakes, the 10-fold cross-validation is also utilised in the model training process. Table 6 displays the evaluation findings for each model, and it is clear that SRXGWO-SVR performs the best in terms of R^2 , RMSE, and MAE assessment indices. The correlation coefficient, R^2 , is 0.99879, which shows that there is a strong connection between the prediction results of the SRXGWO-SVR model and the actual value. It is clear that SRXGWO-SVR performs best in R^2 , RMSE, and MAE evaluation indices. RMSE and MAE are used to evaluate errors. The two forms of SVR errors are the least, with corresponding values of 159.5753 and 100.0009. Following line graph analysis, iterative graph analysis, and evaluation result analysis, it can be shown that the SRXGWO-SVR model has a very high prediction accuracy and also has more advantages than other

Table 6
Evaluation results of each prediction model.

Model	R^2	RMSE	MAE
SRXGWO-SVR	0.99879	159.5753	100.0009
GWO-SVR	0.99869	159.5886	100.0069
SVR	0.99861	166.1568	105.0999
BP	0.99820	584.2596	119.5581
RF	0.98379	176.6171	335.1838
KELM	0.99819	195.6333	144.1484
RBF	0.99865	168.8734	110.3226
CNN	0.99744	228.9898	110.3226

algorithms.

2. Prediction experiments on the test set

The model trained by the real sequence must be closer to the training set itself, and there may be problems of false accuracy of the prediction results and overfitting of the prediction model. Moreover, the prediction problem, in reality, will not be the same as the real sequence of the training set, so it is necessary to simulate and test the completed trained model by the test set.

Fig. 8 shows the prediction fold of SRXGWO-SVR for the test set. Again, the Original fold represents the data distribution of the test set, and the Predicted fold represents the prediction results given by the SRXGWO-SVR model. It can be seen that SRXGWO-SVR also predicts very well in the test set prediction with high correlation. However, the deviation of SRXGWO-SVR in predicting the test set is more significant than the training set, e.g., the deviation of the dashboard on days 7, 10, 13, 36 is larger. Therefore, overall, SRXGWO-SVR still has a highly accurate prediction performance and does not fall into the overfitting problem when faced with brand-new patient-flow data. However, it cannot achieve the results in training.

To further explore the performance of SRXGWO-SVR in the face of new sample sequences and to show the advantages of SRXGWO-SVR over other algorithms, the test set experiments also compare SRXGWO-SVR with well-known classification prediction models such as GWO-SVR, SVR, and BP, and evaluate the prediction results using R^2 , RMSE, and MAE. The evaluation results of each model are shown in **Table 7**. It can be seen that SRXGWO-SVR has higher Spearman correlation and lower error in RMSE, MAE for prediction results compared with GWO-SVR, SVR, which indicates that SRXGWO-SVR still has an advantage over the unimproved GWO-SVR and SVR in the face of new data sets. In addition, it can be seen that SRXGWO-SVR still has a greater advantage over BP, RF, KELM, RBF, and CNN classical models, and performs better in terms of R^2 , RMSE, and MAE.

Finally, this paper combines the prediction results of the training set and the test set for statistical comparisons in order to further highlight the significance of the training set experiments and the test set experiments, as well as to demonstrate the prediction effectiveness of SRXGWO-SVR for various data sets and the advantages of SRXGWO-SVR over other algorithms. The comparison findings are shown in **Figs. 9–11**, where the horizontal axis represents each comparison model and the vertical axis the assessment standards. **Fig. 9** shows that when SRXGWO-

Table 7
Evaluation results of each model based on the test set.

Model	R^2	RMSE	MAE
SRXGWO-SVR	0.99835	199.0553	125.6847
GWO-SVR	0.99802	199.0954	125.7070
SVR	0.99783	218.1971	136.1934
BP	0.99738	232.2147	150.2261
RF	0.97952	701.2146	427.7865
KELM	0.99819	291.1310	185.8860
RBF	0.99831	201.5883	129.3960
CNN	0.98132	628.8679	363.9654

SVR is moved from the training set to the test set, the prediction relevance of the model diminishes and that KELM fluctuates the least. However, SRXGWO-SVR still outperforms KELM in terms of accuracy, suggesting that it may continue to hold the top spot in future patient-flow prediction. The assessment findings were normalized in this research and then shown once more since RMSE and MAE are prediction errors and the difference between the data is too great. **Figs. 10 and 11** show intuitively how much more accurate SRXGWO-SVR is than other models like BP, RF, CNN, and others. Additionally, even after switching datasets, there is little error variation in the SRXGWO-SVR prediction results, demonstrating the model's great stability. It can be shown that SRXGWO-SVR is a very accurate, highly generalizable, and highly stable prediction model based on the experimental findings of the training and test sets.

5. Conclusions and future works

This paper proposes a high-performance optimization algorithm SRXGWO and an effective patient-flow prediction model SRXGWO-SVR, aiming to predict patients' medical needs and achieve orderly patient access by analyzing the changing dynamics and objective laws of Patient-flow. First, this paper introduces the current research status of artificial intelligence technology for predicting patient-flow and finds that the existing prediction models are not strong in prediction accuracy and generalization. Therefore, to improve the accuracy and generalization of the prediction model, SRXGWO is proposed based on three improvement strategies and GWO, in which the Sobol sequence improves the solution space coverage of population initialization, Cauchy random replacement strategy enhances the information exchange between individuals, directional mutation mechanism improves the search

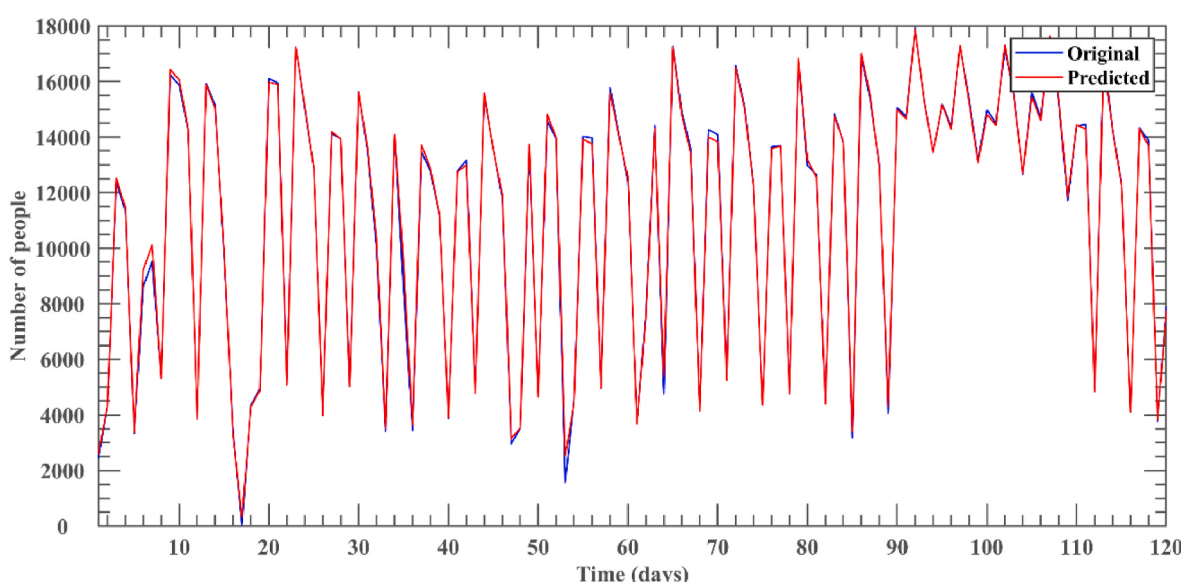


Fig. 8. SRXGWO-SVR predictions for the test set.

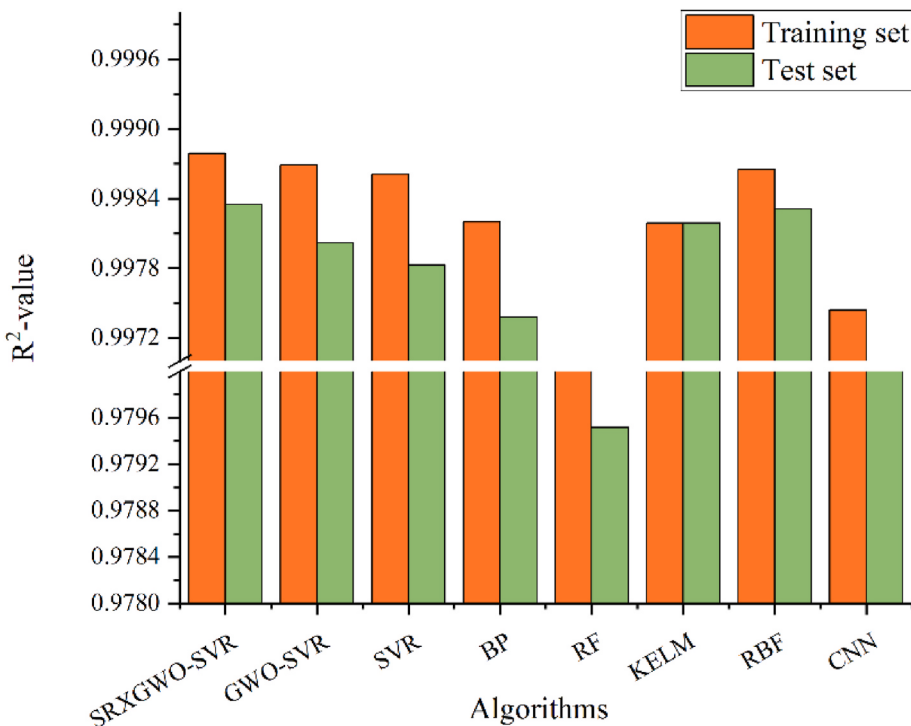


Fig. 9. R^2 comparison results based on two dataset models.

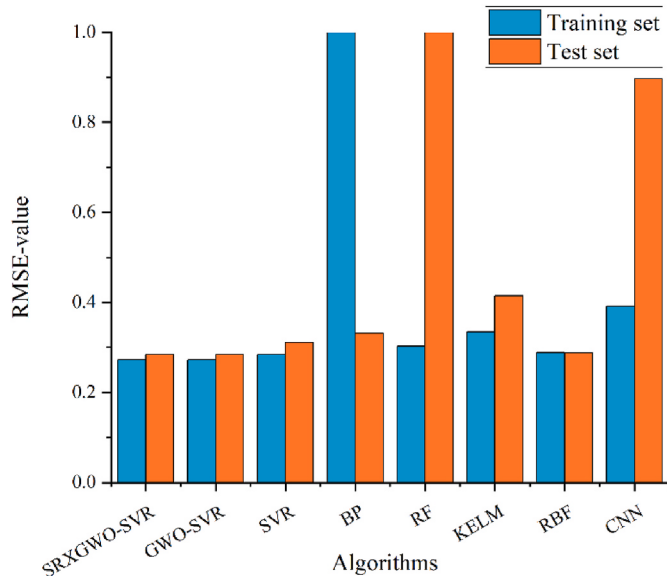


Fig. 10. Comparison results of RMSE based on two dataset models.

ability of the algorithm and the ability to jump out of the local optimum. Then, the SRXGWO-SVR prediction model is proposed by combining the high-performance SRXGWO algorithm with the SVR prediction method to accurately predict the number of patients and reasonably schedule medical resources. In the experimental part, ablation experiments are first conducted to compare SRXGWO with GWO combined with different mechanisms. It is verified that SRXGWO, with three improved strategies, simultaneously is the strongest performance. Then, SRXGWO is compared with 12 highly cited algorithms, such as PSO, SCA, etc., by 30 benchmark functions to demonstrate that SRXGWO is also superior in the search ability and exploitation ability of peer algorithms. Finally, a real patient-flow dataset is used to validate the prediction ability of the

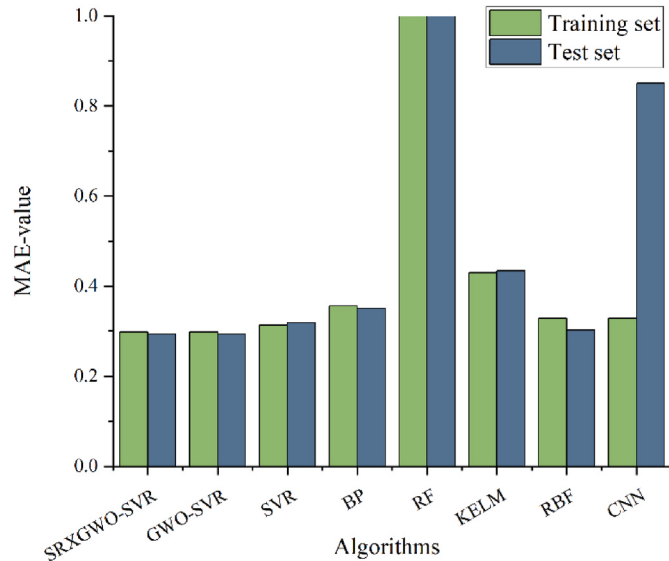


Fig. 11. Comparison results of MAE based on two dataset models.

SRXGWO-SVR model. Comparing with the other seven prediction models, such as BP, CNN, etc., and evaluating R^2 , RMSE, and MAE, it is proved that the prediction results of SRXGWO-SVR are more accurate, effective and stronger than other models.

Of course, the research in this paper also has some limitations. For example, three improvement mechanisms were added to GWO, which increased the algorithm's complexity. In the future, we will try to solve this problem using parallel techniques and high-performance computers. In addition, in future work, we will further enhance SRXGWO and SRXGWO-SVR and apply them to more fields.

Declaration of competing interest

The authors declare that there is no conflict of interests regarding the publication of article.

References

- [1] L. Zhang, L. Li, Study on the Equilibrium of Spatial Allocation of Medical Resources at Different Levels in Shanghai, *Urban Studies*, 2019, p. 26.
- [2] D.Y. Zhou, L.Y. Gao, Q.H. Pan, M.F. He, The Impacts of Medical Resources on Emerging Self-Limiting Infectious Diseases, vol. 12, Applied Sciences-Basel, 2022.
- [3] H. Li, D.M. Mu, P. Wang, Y. Li, D.X. Wang, Prediction of obstetric patient flow and horizontal allocation of medical resources based on time series analysis, *Front. Public Health* 9 (2021).
- [4] A. Nikakhtar, S.A. Abbasian-Hosseini, H. Gazula, S.M. Hsiang, Social Network based sensitivity analysis for patient flow using computer simulation, *Comput. Ind. Eng.* 88 (2015) 264–272.
- [5] A.R. Sharafat, M. Bayati, PatientFlowNet: a deep learning approach to patient flow prediction in emergency departments, *IEEE Access* 9 (2021) 45552–45561.
- [6] M. Tavakoli, R. Tavakkoli-Moghaddam, R. Mesbahi, M. Ghanavati-Nejad, A. Tajally, Simulation of the COVID-19 patient flow and investigation of the future patient arrival using a time-series prediction model: a real-case study, *Med. Biol. Eng. Comput.* 60 (2022) 969–990.
- [7] S. Mirjalili, S.M. Mirjalili, A. Lewis, Grey wolf optimizer, *Adv. Eng. Software* 69 (2014) 46–61.
- [8] X.-S. Yang, A new metaheuristic bat-inspired algorithm, in: J.R. González, D. A. Pelta, C. Cruz, G. Terrazas, N. Krasnogor (Eds.), *Nature Inspired Cooperative Strategies for Optimization (NISCO 2010)*, Springer Berlin Heidelberg, Berlin, Heidelberg, 2010, pp. 65–74.
- [9] R. Storn, K.J.J.o.G.O. Price, Differential evolution – a simple and efficient heuristic for global, Optimization over Continuous Spaces 11 (1997) 341–359.
- [10] S. Mirjalili, SCA, A Sine Cosine Algorithm for solving optimization problems, *Knowl. Base Syst.* 96 (2016) 120–133.
- [11] S. Mirjalili, A.H. Gandomi, S.Z. Mirjalili, S. Saremi, H. Faris, S.M. Mirjalili, Salp Swarm Algorithm: a bio-inspired optimizer for engineering design problems, *Adv. Eng. Software* 114 (2017) 163–191.
- [12] S. Mirjalili, A. Lewis, The whale optimization algorithm, *Adv. Eng. Software* 95 (2016) 51–67.
- [13] S. Mirjalili, Moth-flame optimization algorithm: a novel nature-inspired heuristic paradigm, *Knowl. Base Syst.* 89 (2015) 228–249.
- [14] J. Kennedy, R. Eberhart, Particle swarm optimization, in: Proceedings of ICNN'95 vol. 1944, International Conference on Neural Networks, 1995, pp. 1942–1948.
- [15] Y. Yang, H. Chen, A.A. Heidari, A.H. Gandomi, Hunger games search: visions, conception, implementation, deep analysis, perspectives, and towards performance shifts, *Expert Syst. Appl.* 177 (2021), 114864.
- [16] A.A. Heidari, S. Mirjalili, H. Faris, I. Aljarah, M. Mafarja, H. Chen, Harris hawks optimization algorithm and applications, Future Generation Computer Systems-the International Journal of Escience 97 (2019) 849–872.
- [17] H. Su, D. Zhao, A. Asghar Heidari, L. Liu, X. Zhang, M. Mafarja, H. Chen, RIME: A Physics-Based Optimization, *Neurocomputing*, 2023.
- [18] J. Tu, H. Chen, M. Wang, A.H. Gandomi, The colony predation algorithm, *Journal of Bionic Engineering* 18 (2021) 674–710.
- [19] I. Ahmadianfar, A. Asghar Heidari, A.H. Gandomi, X. Chu, H. Chen, RUN beyond the metaphor: an efficient optimization algorithm based on Runge Kutta method, *Expert Syst. Appl.* (2021), 115079.
- [20] I. Ahmadianfar, A. Asghar Heidari, S. Noshadian, H. Chen, A.H. Gandomi, INFO: an efficient optimization algorithm based on weighted mean of vectors, *Expert Syst. Appl.* (2022), 116516.
- [21] H. Chen, C. Li, M. Mafarja, A.A. Heidari, Y. Chen, Z. Cai, Slime mould algorithm: a comprehensive review of recent variants and applications, *Int. J. Syst. Sci.* (2022) 1–32.
- [22] S. Li, H. Chen, M. Wang, A.A. Heidari, S. Mirjalili, Slime mould algorithm: a new method for stochastic optimization, *Future Generat. Comput. Syst.* 111 (2020) 300–323.
- [23] M. Abd Elaziz, D. Oliva, S. Xiong, An improved opposition-based sine cosine algorithm for global optimization, *Expert Syst. Appl.* 90 (2017) 484–500.
- [24] C. Qu, Z. Zeng, J. Dai, Z. Yi, W. He, A modified sine-cosine algorithm based on neighborhood search and greedy Levy mutation, *Comput. Intell. Neurosci.* (2018), 2018(4231647–4231647).
- [25] A.A. Heidari, R. Ali Abbaspour, H. Chen, Efficient boosted grey wolf optimizers for global search and kernel extreme learning machine training, *Appl. Soft Comput.* 81 (2019), 105521.
- [26] M.A. Elhosseini, A.Y. Haikal, M. Badawy, N. Khashan, Biped robot stability based on an A-C parametric Whale Optimization Algorithm, *Journal of Computational Science* 31 (2019) 17–32.
- [27] H. Chen, S. Li, A.A. Heidari, P. Wang, J. Li, Y. Yang, M. Wang, C. Huang, Efficient multi-population outpost fruit fly-driven optimizers: framework and advances in support vector machines, *Expert Syst. Appl.* (2020) 142.
- [28] H. Nenavath, R.K. Jatoth, Hybridizing sine cosine algorithm with differential evolution for global optimization and object tracking, *Appl. Soft Comput.* 62 (2018) 1019–1043.
- [29] Y. Zhang, R. Liu, A.A. Heidari, X. Wang, Y. Chen, M. Wang, H. Chen, Towards augmented kernel extreme learning models for bankruptcy prediction: algorithmic behavior and comprehensive analysis, *Neurocomputing* 430 (2021) 185–212.
- [30] Y. Liu, A.A. Heidari, Z. Cai, G. Liang, H. Chen, Z. Pan, A. Alsufyani, S. Bourouis, Simulated annealing-based dynamic step shuffled frog leaping algorithm: optimal performance design and feature selection, *Neurocomputing* 503 (2022) 325–362.
- [31] Y. Xue, B. Xue, M. Zhang, Self-adaptive particle swarm optimization for large-scale feature selection in classification, *ACM Trans. Knowl. Discov. Data* 13 (2019) 1–27.
- [32] Y. Xue, X. Cai, F. Neri, A multi-objective evolutionary algorithm with interval based initialization and self-adaptive crossover operator for large-scale feature selection in classification, *Appl. Soft Comput.* 127 (2022), 109420.
- [33] X. Wang, X. Dong, Y. Zhang, H. Chen, Crisscross Harris hawks optimizer for global tasks and feature selection, *Journal of Bionic Engineering* (2022) 1–22.
- [34] W. Shan, H. Hu, Z. Cai, H. Chen, H. Liu, M. Wang, Y. Teng, Multi-strategies boosted mutative crow search algorithm for global tasks: cases of continuous and discrete optimization, *Journal of Bionic Engineering* 19 (2022) 1830–1849.
- [35] R. Dong, H. Chen, A.A. Heidari, H. Turabieh, M. Mafarja, S. Wang, Boosted kernel search: framework, analysis and case studies on the economic emission dispatch problem, *Knowl. Base Syst.* 233 (2021), 107529.
- [36] C. Zhao, Y. Zhou, X. Lai, An integrated framework with evolutionary algorithm for multi-scenario multi-objective optimization problems, *Inf. Sci.* 600 (2022) 342–361.
- [37] W. Deng, J. Xu, X.Z. Gao, H. Zhao, An enhanced MSIQDE algorithm with novel multiple strategies for global optimization problems, *IEEE Transactions on Systems, Man, and Cybernetics: Systems* 52 (2022) 1578–1587.
- [38] G. Sun, R. Han, L. Deng, C. Li, G. Yang, Hierarchical Structure-Based Joint Operations Algorithm for Global Optimization, *Swarm and Evolutionary Computation*, 2023, 101311.
- [39] K. Yu, D. Zhang, J. Liang, K. Chen, C. Yue, K. Qiao, L. Wang, A correlation-guided layered prediction approach for evolutionary dynamic multiobjective optimization, *IEEE Trans. Evol. Comput.* (2022), 1–1.
- [40] G. Sun, G. Yang, G. Zhang, Two-level parameter cooperation-based population regeneration framework for differential evolution, *Swarm Evol. Comput.* 75 (2022), 101122.
- [41] C. Li, G. Sun, L. Deng, L. Qiao, G. Yang, A population state evaluation-based improvement framework for differential evolution, *Inf. Sci.* 629 (2023) 15–38.
- [42] G. Sun, C. Li, L. Deng, An adaptive regeneration framework based on search space adjustment for differential evolution, *Neural Comput. Appl.* 33 (2021) 9503–9519.
- [43] X. Wen, K. Wang, H. Li, H. Sun, H. Wang, L. Jin, A two-stage solution method based on NSGA-II for Green Multi-Objective integrated process planning and scheduling in a battery packaging machinery workshop, *Swarm Evol. Comput.* 61 (2021), 100820.
- [44] G. Wang, E. Fan, G. Zheng, K. Li, H. Huang, Research on Vessel Speed Heading and Collision Detection Method Based on AIS Data, *Mobile Information Systems*, 2022.
- [45] Y. Xue, Y. Tong, F. Neri, An ensemble of differential evolution and Adam for training feed-forward neural networks, *Inf. Sci.* 608 (2022) 453–471.
- [46] J. Chen, Z. Cai, H. Chen, X. Chen, J. Escoria-Gutierrez, R.F. Mansour, M. Ragab, Renal pathology images segmentation based on improved cuckoo search with diffusion mechanism and adaptive beta-hill climbing, *Journal of Bionic Engineering* (2023).
- [47] Y. Han, W. Chen, A.A. Heidari, H. Chen, Multi-verse optimizer with rosenbrock and diffusion mechanisms for multilevel threshold image segmentation from COVID-19 chest X-ray images, *Journal of Bionic Engineering* 20 (2023) 1198–1262.
- [48] J. Xing, H. Zhao, H. Chen, R. Deng, L. Xiao, Boosting whale optimizer with quasi-oppositional learning and Gaussian barebone for feature selection and COVID-19 image segmentation, *Journal of Bionic Engineering* 20 (2023) 797–818.
- [49] H. Hu, W. Shan, J. Chen, L. Xing, A.A. Heidari, H. Chen, X. He, M. Wang, Dynamic individual selection and crossover boosted forensic-based investigation algorithm for global optimization and feature selection, *Journal of Bionic Engineering* (2023).
- [50] X. Wang, X. Dong, Y. Zhang, H. Chen, Crisscross Harris hawks optimizer for global tasks and feature selection, *Journal of Bionic Engineering* 20 (2023) 1153–1174.
- [51] C. Lin, P. Wang, A.A. Heidari, X. Zhao, H. Chen, A boosted communicational salp swarm algorithm: performance optimization and comprehensive analysis, *Journal of Bionic Engineering* 20 (2023) 1296–1332.
- [52] C. Lin, P. Wang, X. Zhao, H. Chen, Double mutational salp swarm algorithm: from optimal performance design to analysis, *Journal of Bionic Engineering* 20 (2023) 184–211.
- [53] J. Hu, S. Lv, T. Zhou, H. Chen, L. Xiao, X. Huang, L. Wang, P. Wu, Identification of pulmonary hypertension animal models using a new evolutionary machine learning framework based on blood routine indicators, *Journal of Bionic Engineering* 20 (2023) 762–781.
- [54] J. Liang, K. Qiao, C. Yu, B. Qu, C. Yue, W. Guo, L. Wang, Utilizing the relationship between unconstrained and constrained pareto fronts for constrained multiobjective optimization, *IEEE Trans. Cybern.* (2022) 1–14.
- [55] C. Huang, X. Zhou, X. Ran, Y. Liu, W. Deng, W. Deng, Co-evolutionary competitive swarm optimizer with three-phase for large-scale complex optimization problem, *Inf. Sci.* 619 (2023) 2–18.
- [56] J.S. Chou, J.P.P. Thedja, Metaheuristic optimization within machine learning-based classification system for early warnings related to geotechnical problems, *Autom. ConStruct.* 68 (2016) 65–80.
- [57] A. Kaushik, N. Singal, A hybrid model of wavelet neural network and metaheuristic algorithm for software development effort estimation, *Int. J. Inf. Technol.* 14 (2022) 1689–1698.
- [58] M. Mehraein, A. Mohanavelu, S.R. Naganna, C. Kulls, O. Kisi, Monthly Streamflow Prediction by Metaheuristic Regression Approaches Considering Satellite Precipitation Data, vol. 14, *Water*, 2022.

- [59] K. Zhu, S. Ying, N.N. Zhang, D.D. Zhu, Software defect prediction based on enhanced metaheuristic feature selection optimization and a hybrid deep neural network, *J. Syst. Software* 180 (2021).
- [60] J.S. Chou, K.H. Yang, J.P. Pampang, P. Anh-Duc, Evolutionary metaheuristic intelligence to simulate tensile loads in reinforcement for geosynthetic-reinforced soil structures, *Comput. Geotech.* 66 (2015) 1–15.
- [61] J.W. Ma, D. Xia, H.X. Guo, Y.K. Wang, X.X. Niu, Z.Y. Liu, S. Jiang, Metaheuristic-based support vector regression for landslide displacement prediction: a comparative study, *Landslides* 19 (2022) 2489–2511.
- [62] N.D. Hoang, D.T. Bui, L. Kuo-Wei, Groutability estimation of grouting processes with cement grouts using differential flower pollination optimized support vector machine, *Appl. Soft Comput.* 45 (2016) 173–186.
- [63] S. García, A. Fernández, J. Luengo, F. Herrera, Advanced nonparametric tests for multiple comparisons in the design of experiments in computational intelligence and data mining: experimental analysis of power, *Inf. Sci.* 180 (2010) 2044–2064.
- [64] J. Derrac, S. García, D. Molina, F. Herrera, A practical tutorial on the use of nonparametric statistical tests as a methodology for comparing evolutionary and swarm intelligence algorithms, *Swarm Evol. Comput.* 1 (2011) 3–18.
- [65] C. Zhao, H. Wang, H. Chen, W. Shi, Y. Feng, JAMSNNet: a remote pulse extraction network based on joint attention and multi-scale fusion, *IEEE Trans. Circ. Syst. Video Technol.* (2022), 1–1.
- [66] J. Lv, G. Li, X. Tong, W. Chen, J. Huang, C. Wang, G. Yang, Transfer learning enhanced generative adversarial networks for multi-channel MRI reconstruction, *Comput. Biol. Med.* 134 (2021), 104504.
- [67] X. Xue, G. Li, D. Zhou, Y. Zhang, L. Zhang, Y. Zhao, Z. Feng, L. Cui, Z. Zhou, X. Sun, Research roadmap of service ecosystems: a crowd intelligence perspective, *International Journal of Crowd Science* 6 (2022) 195–222.
- [68] X. Xue, X.-N. Yu, D.-Y. Zhou, X. Wang, Z.-B. Zhou, F.-Y. Wang, Computational Experiments: Past, Present and Future, 2022 arXiv preprint arXiv:2202.13690.
- [69] X. Xue, X. Yu, D. Zhou, C. Peng, X. Wang, D. Liu, F.-Y. Wang, Computational experiments for complex social systems—Part III: the docking of domain models, *IEEE Transactions on Computational Social Systems* (2023).
- [70] X. Cao, T. Cao, Z. Xu, B. Zeng, F. Gao, X. Guan, Resilience constrained scheduling of mobile emergency resources in electricity-hydrogen distribution network, *IEEE Trans. Sustain. Energy* (2022) 1–15.
- [71] Y. Dai, J. Wu, Y. Fan, J. Wang, J. Niu, F. Gu, S. Shen, MSEva: a musculoskeletal rehabilitation evaluation system based on EMG signals, *ACM Trans. Sens. Netw.* 19 (2022) 1–23.
- [72] J. Zhou, X. Zhang, Z. Jiang, Recognition of imbalanced epileptic EEG signals by a graph-based extreme learning machine, *Wireless Commun. Mobile Comput.* 2021 (2021), 5871684.